

Structural framework and timing of the Pahtohavare Cu ± Au deposits, Kiruna mining district, Sweden

Leslie Logan¹, Ervin Veress¹, Joel B.H. Andersson¹, Olof Martinsson¹, Tobias E. Bauer¹

¹Division of Geosciences and Environmental Engineering, Luleå University of Technology, Luleå SE-971 87, Sweden

5 *Correspondence to:* Leslie Logan (Leslie.logan@ltu.se)

Abstract. As part of a larger mineral systems approach to Cu-bearing mineralization in northern Norrbotten, this study utilizes structural geology to set the classic Pahtohavare Cu ± Au deposits into an up-to-date tectonic framework. The Pahtohavare Cu ± Au deposits, situated only 5 km SW of the Kiirunavaara world-class iron oxide-apatite (IOA) deposit, have a dubious timing and their link to IOA formation is not constrained. The study area contains both epigenetic Cu ± Au (Pahtohavare) and iron oxide-copper-gold (IOCG, Rakkurijärvi) mineral occurrences which are hosted in bedrock that has been folded and bound by two shear zones trending NE-SW and NW-SE to the east and southwest, respectively. Structural mapping and petrographic investigation of the area reveal an ~~anti~~antiform, noncylindrical, SE-plunging ~~fold geometry~~anticline. The cleavage measurements mirror the fold geometry which characterizes the fold as F₂ associated to the late phase of the Svecokarelian orogeny. Porphyroclasts with pressure shadows, ~~and~~ mylonitic fabrics, ~~and foliation trails in porphyroblasts observed in thin section~~ indicate S₀/S₁ is a tectonic fabric. The epigenetic Pahtohavare Cu ± Au mineralization sit in brittle-ductile structures that cross cut an earlier foliation and the F₂ fold, indicating that the timing of the deposits occurred syn- to post-F₂ folding, at least ca. 80 Myr after the Kiirunavaara IOA formation. A 3D model and cross sections of the Pahtohavare-Rakkurijärvi area and a new structural framework of the district are presented and used to suggest that the shear zones bounding the area are likely reactivated early structures that have played a critical role in ore formation in the Kiruna mining district.

20 1 Introduction

Globally, there has been a growing interest in research on clarifying the genetic relationship between iron oxide-apatite (IOA) and iron oxide-copper-gold (IOCG) deposits. Several studies from the Chilean iron belt, the Great Bear Magmatic Zone, and the St. Francois Mountains terrane in SE Missouri argue that IOA and IOCG deposits form from a single evolving magmatic-hydrothermal or hydrothermal fluid during one ore-forming event (cf. Corriveau et al., 2016; Day et al., 2016; Barra et al., 2017; Simon et al., 2018), building on the concept that IOA deposits may represent the deeper roots of a spectrum between an IOA-IOCG mineral system (Sillitoe, 2003). However, other researchers argue that these two deposit types have distinct geneses despite sharing similar geologic environments and characteristics (e.g. Williams et al., 2005; Groves et al., 2010; Tornos, 2011; Barton, 2014; Martinsson et al., 2016; Skirrow, 2021). For example, some researchers favor a purely orthomagmatic model for IOA deposits (e.g. Nyström and Henriquez, 1994; Naslund et al., 2002; Velasco et al., 2016; Tornos et al., 2017; Troll et

30 [al., 2019](#)), a model that is incongruous for some IOCG deposits in which a magmatic-hydrothermal fluid and/or metal source is indirect or ambiguous (c.f. [Barton, 2014](#)).

The Kiruna mining district is situated in the northern Norrbotten ore province ([Martinsson et al., 2016](#)) which has abundant Fe and Cu-Au mineralization, extensive Na-Ca metasomatism ([Frietsch et al., 1997](#)), and regional crustal-scale fault structures ([Bergman et al., 2001](#)). Multiple styles of mineralization are hosted in Rhyacian to Orosirian rocks with major ore forming periods related to the Orosirian Svecokarelian orogeny (ca. 1.9 to 1.8 Ga; [Bergman et al., 2001](#); [Martinsson et al., 2016](#)). The orogeny was polyphase and resulted in complex reactivation of structures and overprinting metamorphic events, alteration assemblages, ~~metamorphic events, structures,~~ and mineralization regionally (e.g. [Wright, 1988](#); [Bergman et al., 2001](#); [Wanhainen et al., 2012](#); [Martinsson et al., 2016](#); [Bergman, 2018](#); [Andersson et al., 2021](#); [Bauer et al., 2022](#)). Radiometric studies point to abundant ~~iron oxide-apatite (IOA)~~ and Cu-Au mineralization processes during the early orogenic phase of the Svecokarelian orogeny (ca. 1880-1860 Ma; [Cliff et al., 1990](#); [Romer et al., 1994](#); [Wanhainen et al., 2005](#); [Smith et al., 2007](#), 2009; [Westhues et al., 2016](#); [Martinsson et al., 2016](#)), however increasing structural evidence links a generation of Cu ± Au mineralization to brittle structures constrained to a late phase of the tectonic evolution ([Bauer et al., 2018, 2022](#); [Andersson et al., 2020, 2021](#)), supported by radiometric studies ([Storey et al., 2007](#); [Martinsson et al., 2016](#); [Sarlus et al., 2018](#); [Andersson et al., 2022](#)). [For example, Bauer et al. \(2018, 2022\) use structural constraints on alteration and mineralization to show Cu-Au mineralization in the Nautanen deformation zone and the Malmberget IOA deposit are hosted in late orogenic structures, and they suggest that either a late mineralization with new metal input occurred, or that tectonically late structures acted as traps for remobilized metals.](#) These findings raise an important question about the relative timing of Cu ± Au introduction and/or remobilization in the Norrbotten ore province and how IOA mineralizing systems are related to Cu-Au occurrences in the context of the tectonic evolution. ~~A well characterized regional structural framework offers a tool for unraveling the relative timing of events where multiple generations of similar alteration and mineralization styles may overprint each other, where isotopic systems used for radiometric dating are subject to disturbance, or where datable phases in relevant textural positions are lacking.~~

In the southern Kiruna mining district, structurally and lithologically controlled, stratabound to discordant Cu ± Au deposits are known in the Pahtohavare area ([Martinsson et al., 1997a](#)) and occur ca. 2 km northwest of the Rakkurijärvi iron oxide-copper-gold (IOCG) deposit. These Fe ± Cu ± Au deposits are situated 5 km SW of the world-class Kiirunavaara IOA deposit which has received over a hundred years of scientific spotlight (e.g. [Geijer, 1910](#); [Lundbohm, 1910](#); [Parák, 1975](#); [Cliff et al., 1990](#); [Cliff and Rickard, 1992](#); [Nyström and Henriquez, 1994](#); [Westhues et al., 2016](#)) while the Fe ± Cu ± Au occurrences in the district have relatively few dedicated studies (e.g. [Viscaria, Rakkurijärvi, Pahtohavare; Lindblom et al., 1996](#); [Martinsson et al., 1997](#); [Storey-Smith et al., 2007](#)). [The Kiirunavaara IOA deposit has an accepted age of ca. 1880 Ga \(Welin, 1987; Cliff et al., 1990; Romer et al., 1994; Smith et al., 2009; Westhues et al., 2016; Martinsson et al., 2016\) and has been structurally constrained to the early extensional phase of the Svecokarelian orogeny \(Andersson et al., 2021\), however, the timing and structural setting of the Pahtohavare deposits are unknown. The main purpose of this study is to determine the relative timing of the formation of the Pahtohavare Cu ± Au deposits by conducting a structural investigation of the area and contextualizing](#)

65 the results within the district and regional tectonic frameworks as a part of a broader mineral systems approach (Wyborn et al., 1994). A well-characterized regional structural framework offers a tool for unraveling the relative timing of events where multiple generations of similar alteration and mineralization styles may overprint each other, where isotopic systems used for radiometric dating are subject to disturbance, or where datable phases in relevant textural positions are lacking. The results from this work add important data to the debate about the genesis of IOA and IOCG deposits and whether they necessarily form coevally and under the same tectonic conditions. Furthermore, increased understanding of the timing and structural setting of Cu ± Au deposits in Norrbotten is important for exploration. This study will add significant new data from the southern Kiruna mining district where limited structural information has been published (Martinsson et al., 1993).

70 Globally, there has been a growing interest in research on clarifying the genetic relationship between IOA and IOCG deposits. Several studies from the Chilean iron belt, the Great Bear Magmatic Zone, and the St. Francois Mountains terrane in SE Missouri argue that IOA and IOCG deposits form from a single evolving magmatic-hydrothermal or hydrothermal fluid during one ore-forming event (cf. Corriveau et al., 2016; Day et al., 2016; Barra et al., 2017; Simon et al., 2018), building on the concept that IOA deposits may represent the deeper roots of a spectrum between an IOA-IOCG mineral system (Sillitoe, 2003). However, other researchers argue that these two deposit types have distinct geneses despite sharing similar geologic environments and characteristics (e.g. Williams et al., 2005; Groves et al., 2010; Tornos, 2011; Barton, 2014; Martinsson et al., 2016; Skirrow, 2021). For example, some researchers favor a purely orthomagmatic model for IOA deposits (e.g. Nyström and Henriquez, 1994; Naslund et al., 2002; Velasco et al., 2016; Tornos et al., 2017; Troll et al., 2019); a model that is incongruous for some IOCG deposits in which a magmatic-hydrothermal fluid and/or metal source is indirect or ambiguous (e.f. Barton, 2014).

80 In this study, a structural investigation was conducted in the southern part of the Kiruna mining district where Cu ± Au occur with iron oxides (the Pahtohavare and Rakkurijärvi deposits) as a part of a broader mineral systems approach (Wyborn et al., 1994). The area is not significantly metamorphosed making it an optimal location for depiction of the structural context between IOA and IOCG-style mineralization. The structural results are constrained by a regional tectonic framework and used to illuminate the relative timing of the Pahtohavare Cu ± Au mineralization.

2 Geological Setting

90 The descriptions of the rocks used in this paper follows the nomenclature presented by Martinsson (2004). The rocks in northern Sweden (Fig. 1) are variably metamorphosed from greenschist to amphibolite facies conditions however, the “meta”-prefix is excluded for clarity and emphasis on the original protolith.

Formatted: Font: (Default) +Headings (Times New Roman)

Formatted: Font: (Default) +Headings (Times New Roman)

2.1 Regional geologic setting

2.1.1 Neoproterozoic buildup and early Paleoproterozoic rifting

95 The Norrbotten craton basement rocks comprise ~~of~~ Neoproterozoic (ca. 2.9-2.6 Ga) gneissic granitoids of tonalitic to granodioritic composition, amphibolites, and paragneisses (Martinsson et al., 1999; Bergman et al., 2001) which formed during the continental build-up of the Lopian orogeny (Bergman et al., 2001). The southwestern boundary of the Archean crust has been traced using ϵ_{Nd} values in Paleoproterozoic plutonic-volcanic rocks (Öhlander et al., 1993) that broadly define the margin as running from the Bothnian Bay south of Luleå, towards the NW through Jokkmokk, hence, the Luleå-Jokkmokk line (Mellqvist, 1999; Fig. 1).

100 The early Paleoproterozoic marked major rifting events of the basement (~~ca. 2.5-2.0 Ga~~) which created NW-SE oriented first-order structures (Skyttä et al., 2019) which generated ~~of~~ Tholeiitic volcanic and volcanoclastic rocks and rift-related sedimentary successions ~~were generated from ca. 2.5-2.0 Ga and formed~~ forming a greenstone belt that extends today from northern Norway to Russian Karelia (Pharaoh and Pearce, 1984; Martinsson, 1997; Bingen et al., 2015). ~~(Skyttä et al., 2019)~~ The greenstone successions are important hosts for syn- to post-depositional Fe, Cu, and Cu ± Au mineralization regionally (Martinsson et al., 105 2016).

2.1.2 Svecofennian early orogenic extension and crustal shortening

110 Around 1.90 Ga, NE-directed subduction (BABEL Working Group, 1990; Öhlander et al., 1993) and back-arc extension (Pharaoh and Pearce, 1984; Andersson et al., 2021; Bauer et al., 2022) began along the southern margin of the Archean craton, marking the start of the polyphase Svecofennian accretionary orogenic cycle (Bergman et al., 2001). Several ~~deformation, metamorphic, and~~ magmatic events ~~and associated deformation~~ are recorded in the Norrbotten lithotectonic unit accompanied by varying degrees of hydrothermal alteration, ~~metamorphism,~~ and mineralization (c.f. Bergman et al., 2001; Martinsson et al., 2016; Grigull et al., 2018; Luth et al., 2018b; Bauer et al., 2018; 2022; Bergman and Weihed, 2020; Andersson et al., 2020; 2021). The ~~associated resulting~~ magmatic suites are the calc-alkaline to alkali-calcic Haparanda suite-Porphyrite group and Perthite monzonite suite (PMS)-Kiirunavaara group which vary from mafic to felsic rock types in the northern Norrbotten area 115 (Perdahl and Frietsch, 1993; Bergman et al., 2001; Martinsson, 2004; Sarlus et al., 2020; Logan et al., 2022). Abundant Na-Ca metasomatism related to the elevated thermal flux from the intrusive activity and fluids channeling through faults resulted in the formation of albite, marialitic scapolite, magnetite, amphibole, and carbonate (Frietsch et al., 1997; Bergman et al., 2001; Martinsson et al., 2016; Andersson et al., 2020). Early mineral deposits formed during this time include IOA (e.g. Kiirunavaara), porphyry Cu (Au-Ag-Mo) (e.g. Aitik), and IOCG (e.g. Rakkurijärvi; Smith et al., 2007, 2009; Wanhainen et al., 2005; Westhues et al., 2016). 120

The accretion of the Skellefte volcanic arc to the Archean craton to the north (Hietanen, 1975; Skiöld, 1988; Öhlander et al., 1993; Weihed et al., 2002; Bergman and Weihed, 2020; Skyttä et al., 2020) resulted in crustal shortening from ca. 1.88-1.86 Ga (termed D_1 in Norrbotten, but D_2 in the Skellefte district and Överkalix lithotectonic unit; Skyttä et al., 2012; Bergman and

Formatted: Subscript

Formatted: Subscript

Weihed, 2020). ~~The movement along shear zones is less known from this event but kinematic data from approximately 40 km southwest of Kiruna (Fig. 1) suggests that reverse-oblique sinistral movement occurred (Andersson et al., 2020). Structurally, the event is characterized by a~~ penetrative, but heterogeneously developed, dominantly NW-SE striking tectonic fabric ~~development~~formed from an inferred NE-SW shortening direction under mostly plastic conditions (Grigull et al., 2018; Bauer et al., 2018, 2022; Andersson et al., 2020, 2024). The tectonic fabric is interpreted to have formed under peak metamorphic ~~me~~ conditions (lower amphibolite) recorded by syn-tectonic growth of hornblende (Andersson et al. 2020), though regionally the metamorphic grade can be higher (Bergman et al., 2001). Amphibolite facies metamorphism characterizes M_1 in Norrbotten except in the Kiruna mining district which shows a lower overall metamorphic grade characterized by upper greenschist facies metamorphism, though local transitions to lower amphibolite facies occur (Bergman et al., 2001, Andersson et al. 2021; 2022). In the Skellefte district a 1.87 Ga basin inversion is observed (Bauer et al., 2011; Skyttä et al., 2012), however, it is not recorded or is masked in the Kiruna mining district (Andersson et al. 2021).

Formatted: Subscript

2.1.3 Svecokarelian late orogenic crustal shortening

A second phase of subduction initiated around 1.81-1.78 Ga, coeval with abundant crustal melting and emplacement of silica-rich granites of the Lina suite and quartz-poor monzonitic A-/I-type granitoids, syenites, and gabbros of the Transscandinavian Igneous Belt (Bergman et al., 2001; Högdahl et al., 2004; Bergman et al., 2006; Martinsson et al., 2018; Sarlus et al., 2018). Metamorphism has been suggested to be of high temperature, low pressure, high temperature conditions during this orogenic phase due to the occurrence of brittle structures and folding with only locally developed, spaced axial plane-parallel fabric, together with higher temperature minerals (e.g. cordierite, garnet; Bergman et al., 2001; Bauer et al., 2018; Skelton et al., 2018) Bergman et al., 2001; Bauer et al., 2018). Commonly Additionally, K to K-Fe metasomatism/alteration can be found in late orogenic (D_2) shear zones and brittle fractures (Andersson et al., 2020; Bauer et al., 2022) and occurs in spatial proximity to late orogenic intrusions and pegmatites or as a result of late magmatic-hydrothermal activity (Andersson et al., 2020; Bauer et al., 2018; 2022). The second deformation event was inhomogeneous and confined to major deformation zones resulted from E-W crustal shortening (e.g. Bergman et al., 2001; Weihed et al., 2002; Lahtinen et al., 2005; Bauer et al., 2018; Luth et al., 2018b; Andersson et al., 2021). In general, kinematic data show steep east-side-up movement along the shear zones in the east while in the west dominantly west-side-up kinematics are observed (Bergman et al., 2001, Lynch et al., 2015, Luth et al., 2018b, Andersson et al., 2020). The event and is associated with brittle-plastic conditions producing spaced S_2 cleavages and strong strain partitioning (Grigull et al., 2018, Luth et al., 2018b, Bauer et al., 2018; 2022, Andersson et al., 2020). The second phase of deformation This was followed by a clockwise-rotation of the stress field to a NNW-SSE- to N-S-oriented crustal shortening direction (D_3) which caused a gentle refolding of preexisting fabrics and crenulation of white mica and chlorite domains recorded in the Kiruna area (Andersson et al. 2021). A similar direction-orientation of crustal shortening related to D_3 -this deformation event is recorded in the Pajala area to the east, however it differs from that seen in Kiruna by the resultant formation of WNW-ESE and NNW-SSE conjugate faults (Luth et al., 2018a).

Field Code Changed

Formatted: Subscript

Formatted: Subscript

2.1.4 Late Svecokarelian deformation

A late brittle deformation event is observed in both in the Kiruna and in the Gällivare areas (approximately 70 km to the south, Fig. 1) that is characterized by brittle fracturing (Romer, 1996; Bauer et al., 2018; Andersson et al., 2021). At the Luossavaara and Rektor IOA deposits in the Kiruna mining district (Fig. 2), this event is structurally constrained by a calcite-quartz hydraulic breccia that cross cuts S₂ fabrics (Andersson et al., 2021). Furthermore, radiometric U-Pb age constraints on monazite from the Rektor and Kiirunavaara ores identify a late hydrothermal event is identified by radiometric age constraints on monazite from the Rektor and Kiirunavaara ores which yield U-Pb ages of ca. 1.74-1.72 Ga and ca. 1.62 Ga (Blomgren, 2015, LA-ICP-MS; Westhues et al., 2017, SIMS). In Kiruna, U-Pb (SC-ICP-MS) ages from monazite in hydrothermal calcite found in the Kiruna-Naimakka shear zone in central Kiruna show formation at indicates an event at ca. 1.78-1.76 Ga (Lauri et al., 2022). At Malmberget in the Gällivare area (Fig. 1), low-temperature hydrothermal monazite and stilbite associated to late calcite-bearing brittle fractures yield U-Pb crystallization ages between ca. 1.74-1.73 Ga with associated apatite and titanite showing a later recrystallization and/or hydrothermal event around ca. 1.60-1.62 Ga (ID-TIMS, Romer 1996).

2.2 Local geology

2.2.1 Stratigraphy and intrusive rocks

The Kiruna mining district, outlined in Fig. 2, has a well-preserved stratigraphy-lithostratigraphic sequence from Archean to Orosirian age and has previously which has been comprehensively described by Lundbohm (1910), Frietsch et al. (1979), Martinsson et al. (2004), and Andersson et al. (2021). The lowermost part of the sequence includes an Archean granite (ca. 2.7 Ga; Logan et al., 2022) which occurs in a small occurrence. A small occurrence of Archean granite outcrops in the southern part of the district (Fig. 2) and is overlain unconformably overlain by Rhyacian greenstone stratigraphy rocks and later Orosirian rocks (Martinsson, 1997). The lowermost succession of greenstones belongs to the ca. 2.5-2.3 Ga Kovo group, comprising basal clastic sedimentary rocks, basaltic lavas, volcanogenic graywackes, and a series of tholeiitic to calc-alkaline volcanic rocks (Martinsson 1997). Above this unit the Kovo group lies the Kiruna greenstone group which consists of basaltic lavas, conglomerates, and dolostones at the base and that transitions into is overlain by komatiitic to tholeiitic volcanics, tholeiitic to calc-alkaline volcanosedimentary formations, graphite schists, and pillow basalts (Martinsson 1997). with related mafic sills related to the pillow basalt formation occur within the volcanoclastic unit (Martinsson 1997).

The mid-Orosirian rocks related to the early-Svecokarelian orogenic cycle overlie the greenstones with the unconformable Kurravaara conglomerate at the base (Fig. 2). This unit formation is polymictic, poorly sorted, with rounded to subrounded clasts approximately 0.5 to >10 cm (locally up to 50 cm) in size (Frietsch, 1979). A volcanic intercalation in the Kurravaara conglomerate has been radiometrically dated (U-Pb zircon SIMS), which constrains the minimum age of the conglomerate to ca. 1.89 Ga (Andersson et al., 2021). In some areas, andesitic volcanic rocks of the Porphyrite group are the lowermost unit of

the Orosirian stratigraphy; and represent the extrusive products of early arc magmatism (Martinsson and Perdahl, 1995; Martinsson, 2004).

Overlying these basal units are the volcanic rocks of the Kiirunavaara group including the trachyandesitic Hopukka formation and dacitic-rhyolitic Luossavaara formation which make up the footwall and hanging wall, respectively, to the giant Kiirunavaara IOA deposit (Fig. 2; Martinsson 2004). Above the Luossavaara formation The Matojärvi formation overlies the Luossavaara formation and consists of a series of rhyolitic tuffs, basaltic lavas, alluvial breccia-conglomerates, greywackes and phyllites of the Matojärvi formation (Fig. 2; Lundbohm, 1910; Frietsch, 1979; Martinsson, 2004; Andersson et al., 2021) which represents a highly tectonized unit of the stratigraphy (Andersson et al., 2021). This formation is overlain by quartzfeldspar arenites with intercalations of alluvial breccia-conglomerates forming the Hauki quartzite (Fig. 2; Lundbohm 1910, Martinsson 2004).

Distributed through the Kiruna mining district are mafic to felsic plutonic intrusions (Offerberg, 1967) regarded as comagmatic with the Kiirunavaara group (Hopukka and Luossavaara formations) volcanic rocks and suggested to belong to the PMS (Witschard, 1984; Martinsson, 2004). Radiometric dating (U-Pb zircon by ID-TIMS and SIMS) of these intrusions verifies an early orogenic timing (ca. 1.90-1.86 Ga) of magmatic activity (Cliff et al., 1990; Westhues et al., 2016; Logan et al., 2022). Only one U-Pb radiometric determination (ID-TIMS zircon and titanite, 1792 ± 4 Ma) has indicated a late orogenic age for a syenitic intrusion in the district (Romer et al., 1994); however recent geochronological work from the area could not confirm the timing (1880 ± 7 Ma; Logan et al., 2022), making the presence of a late orogenic intrusive body enigmatic (Logan et al., 2022).

2.2.2 Local structures

Structurally, the rock sequence and structural features in the Kiruna mining district strike N to NE and dip steeply to the east. The district lies adjacent to the Kiruna-Naimakka deformation zone (KNDZ) which runs approximately N-S throughout Norrbotten (Fig. 1, 2). Several undulating, approximately N-S- to NE-SW-trending, east-dipping reverse shear zones related to the KNDZ occur parallel to lithostratigraphic boundaries (Andersson et al., 2021) such as at the upper boundary of the Hauki quartzite. East of the Hauki quartzite a thin unit of greenstones is repeated (Fig. 2), a feature also observed in the Rakkurijärvi area. The shear zones show east-side-up kinematics (Andersson et al., 2021) and Structurally, the Kiruna mining district is affected by several periods of tectonic activity. The earliest direct age determination on deformation in the district comes from fracture plane-hosted hydrothermal titanite in an approximately- NNE-SSW trending cataclastic fault damage zone at the Luossavaara IOA deposit (Fig. 2) showing the minimum age of fault initiation to be 1889 ± 26 Ma (Andersson et al., 2022). This is interpreted to represent syn-volcanic faulting during the basin evolution of the early Svecokarelian. The N-S shear zones are interpreted to have been active during the first crustal shortening phase of the Svecokarelian orogeny based on radiometric age results of the Rakkurijärvi IOCG deposit at ca. 1.86 Ga (Re-Os molybdenite and U-Pb LA-ICP-MS allanite, U-Pb TIMS rutile; Smith et al., 2007; 2009; Martinsson et al., 2016); the mineralization for which has been described to be controlled by the adjacent NE-SW trending fault zone (Smith et al., 2007). In the southern Kiruna mining district, the

Formatted: Heading 3

220 Rakkurijärvi IOCG deposit is situated adjacent to a NE-SW trending fault zone that controls the mineralization (Smith et al.,
2007). The deposit was dated (Re-Os molybdenite and U-Pb LA-ICP-MS allanite, U-Pb TIMS rutile) to have formed around
1.86 Ga (Smith et al., 2007; 2009; Martinsson et al., 2016) and suggests the fault was active during the early orogenic crustal
shortening period of the Sveekarelian. Despite evidence of the faults being active at this time, the Orosirian portion of the
stratigraphic sequence in the central Kiruna area (approximately the transect from the Luossavaara IOA deposit through the
225 Hauki quartzite, cf. Andersson et al., 2021; Fig. 2) is reported to lack early orogenic (D₁) deformation fabrics (S₁; Andersson
et al., 2021). The structures in the district and predominantly records late orogenic (D₂) E-W crustal shortening (resulting in
east-side-up kinematics), and basin inversion, and S₂ foliation (Andersson et al., 2021). Strain partitioning commonly
characterizes this event and has resulted in noncoaxial strain focused into lithological contacts and rheologically weak rocks
such as the Matojärvi formation, which represents a high strain zone with highly tectonized and mylonitic rocks (Andersson
230 et al., 2021). In contrast, competent rocks record limited finite strain and have deformed through brittle faulting and fracturing
(Andersson et al., 2021). U-Pb (LA-ICP-MS) age dating on syn-tectonic titanite from a brittle-ductile reverse shear zone with
east-side-up kinematics approximately 6 km east of the Kiirunavaara IOA deposit constrain the age of late Sveekarelian
crustal shortening to between 1812 ± 3 Ma and 1802 ± 8 (Andersson et al., 2021, 2022). Generally east-side-up kinematics are
recovered which are similarly observed in the Kiruna Naimakka deformation zone that runs approximately 5 km to the east of
235 Kiruna (Luth et al. 2018b, Andersson et al. 2021), but contrasting kinematics further north have also been reported (Bergman
et al. 2001).

Following the E-W crustal shortening event, a N-S gentle refolding phase is recorded in the district mainly observed in
crenulated chlorite-white mica domains and in folded fabrics with steep to shallow east-plunging fold axes (Andersson et al.,
2021). This was followed by a late brittle event that cross cuts all earlier fabrics and in the Kiruna mining district is found only
240 locally (Andersson et al., 2021). These include hydraulic fracturing with calcite-quartz infill (Andersson et al., 2021, Lauri et
al., 2022) and remobilization of apatite into veins (Andersson et al., 2021).

2.2.32 Local ore deposits

The Kiruna mining district is host to Kiruna-type IOA deposits and a variety of Cu-mineralization including stratiform-
stratabound Cu (Fe-Zn) deposits (i.e. Viscaria, Eastern Pahtohavare; Martinsson et al., 1997b), epigenetic stratabound to
245 discordant Cu ± Au deposits (Southern, Southeastern, and Central Pahtohavare; Martinsson et al., 1997a), and IOCG-style
deposits (Rakkurijärvi; Smith et al., 2007). While different genetic models exist, thorough structural assessments for of the
copper deposits are lacking.

The area is best known for the giant Kiirunavaara IOA deposit that has been actively mined for iron ore for over a century
(Fig. 2). The deposit is a tabular body of low-Ti magnetite-apatite ore with brecciated hanging and footwall contact zones
250 (Geijer, 1919; Bergman et al., 2001; Martinsson and Hansson, 2004) and is situated along the lithological contact between the
Hopukka and Luossavaara formations. U-Pb radiometric data constrain the timing of the ore formation through the dating of
host rocks, ore minerals, and alteration minerals to ca. 1880 Ma (Welin, 1987; Cliff et al., 1990; Romer et al., 1994; Smith et

al., 2009; Westhues et al., 2016; Martinsson et al., 2016). However, only recently has the structural context of the ore-system been incorporated into a genetic model, with the emplacement of IOA deposits suggested to be coeval with syn-volcanic faulting (1889 ± 26 Ma, titanite U-Pb LA-ICP-MS) during early orogenic basin development and back arc extension (Andersson et al., 2022).

The Rakkurijärvi deposits (ca. 1.86 Ga; Smith et al., 2007; 2009; Martinsson et al., 2016) occur spatially associated to a NE-SW trending shear zone approximately 5 km SSE of the Kiirunavaara IOA (Fig. 2) and have been described to be IOCG-style deposits (Smith et al., 2010). The ore bodies ~~øøøø~~ are hosted in both the Kurravaara conglomerate which occurs to the NW side of the shear zone and in the Kiirunavaara group volcanics (e.g. Hopukka formation) on the SE side (Smith et al., 2007). Chalcopyrite is the main ore bearing sulfide which was precipitated with calcite in the matrix of brecciated massive magnetite and of lithic breccias (Smith et al., 2007). Selective-pervasive magnetite replacement of conglomerate clasts and Cu mineralization within the Kurravaara conglomerate suggests some mineralization is a product of hydrothermal replacement alteration (Smith et al., 2007).

The deposits at Pahtohavare (four sub-localities: Eastern, Southern, Southeastern, and Central, and Eastern, Fig. 2) are situated in the Kiruna greenstone group approximately 5 km SW of the Kiirunavaara IOA. The host stratigraphy rocks are folded into a southeast-plunging anticline with the oldest formations located in the core. They are and truncated on the southwest by a NW-SE trending shear zone (Fig. 2). The kinematics of the shear zone are currently unknown. The earliest mineralization (Eastern Pahtohavare) is suggested to have formed during the deposition of the greenstones (ca. 2.1 Ga) in an exhalative environment based on the stratiform character, alteration in the footwall, and Cu/Zn zonation (Martinsson et al., 1997b). The Southern, Southeastern, and Central Pahtohavare deposits are epigenetic and formed after the deposition of the greenstone Southern rocks. Southern and Southeastern Pahtohavare were mined over a period of seven years during the 1990's and produced 1.7 Mt of ore with 1.9% Cu and 0.9 ppm Au (Martinsson et al., 1997a), and are the main focus of this study, while the ore body at The Central deposit is unmined and dominated by secondary oxidized mineral assemblages.

The epigenetic ore bodies at Southern, Southeastern, and Central are considered epigenetic and are both structurally and lithologically controlled (Martinsson et al., 1997a). ~~Southern and Southeastern Pahtohavare were mined over a period of seven years during the 1990's and produced 1.7 Mt of ore with 1.9% Cu and 0.9 ppm Au (Martinsson et al., 1997a), while the ore body at Central is unmined and dominated by secondary oxidized mineral assemblages.~~ The Southern deposit is situated in the southern limb of the anticline (Fig. 2) and the orebody is bound by tectonic contacts with the geometry being fault-controlled (Martinsson et al., 1997a). However, the mineralization is lithologically constrained to pervasively albite-altered graphite schist and tuffite units (Martinsson et al., 1997a). The ore minerals include chalcopyrite and pyrite disseminated in the albite-altered rocks, as well as in cataclastic and hydrothermal veins and breccia fillings composed of ferro-dolomite-quartz-pyrite-chalcopyrite (Martinsson et al., 1997a). The Southeastern deposit is located in the upper part of the volcanoclastic units of the Kiruna greenstone group (upper Viscaria formation) near the crest of the anticline (Fig. 2; Martinsson et al., 1997a). Lithologically, it is stratabound within pervasively albite-altered mafic-intermediate tuffites and thin graphite schist intercalations but has a distinct NNW-directed subvertical shear zone-with discordant mineralization that cuts the host rocks

290 at a high angle (Martinsson et al., 1997a). The mineralization in the stratabound albite-altered zone occurs disseminated as
chalcopyrite and pyrite and as veinlets and breccia infill. In the discordant ore zone the mineralization occurs in a coarse-
grained ferro-dolomite-quartz-scapolite-albite-chalcopyrite-pyrite vein with mylonitic to cataclastic textures (Martinsson et
al., 1997a). at Southern and Southeastern consists of chalcopyrite and pyrite which occur both disseminated and as breccia
infill in albite-altered graphite schist and tuffite horizons. Pyrite-chalcopyrite also occur in veins of quartz-carbonate in the ore
zone. Occasionally thin magnetite-rich horizons occur within the hosting tuffites (Lindblom et al., 1996; Martinsson et al.,
1997a). The age of the Pahtohavare deposits have not been determined radiometrically, however, they have been
295 suggested to be of a similar age as the Rakkurijärvi deposit based on the geochronological results (1859 ± 2 , U-Pb TIMS) of
rutile taken from a ferrodolomite-pyrite-chalcopyrite vein near the Rakkurijärvi area (Martinsson et al., 2016).

3 Methods

3.1 Geologic mapping and sampling

300 Geologic mapping and structural analysis were carried out between 2019-2021 and during exploration mapping in the early
1990s of the Southeastern Pahtohavare open pit. Approximately 280-300 field measurements were taken from 129-130
localities in the Kiruna mining district field area using a Breithaupt Kassel and Silva compasses. Structural measurements are
reported using the dip/dip azimuth and plunge/azimuth conventions. For magnetite-rich rocks, sighting measurements guided
by known points in the terrain were made with the compass to reduce magnetic-induced errors. For the 2019-2021 field
campaigns, Mmeasurements were digitized directly in the field using the Field Move application (Petroleum Experts Ltd.) on
a ruggedized iPad Mini device. Subsequent structural analyses were performed in the software Move (Petroleum Experts Ltd.).
305 Sampling was conducted in the field and from unoriented drill core at the Geological Survey of Sweden's National Drill Core
Archive in Malå to target structural controls on mineralization. Thirty-seven thin sections were prepared by Precision
Petrographics Ltd. in Vancouver in Canada for petrographic and structural investigation.

3.2 3D Modeling

310 The Pahtohavare-Rakkurijärvi area is relatively less explored compared to the central Kiruna area and the available
observations and measurements are concentrated around the closed open-pit areas. The geological model incorporates the
structural measurements and the geological map from this study, a digital elevation model based on Lantmateriet elevation
data (2+m grid precision), and drill hole lithological logs from 31 holes (open-source data from the Swedish Geological
Survey). In total 6625_m of drill cores were available with an average depth of 214 m. Drill cores were not oriented, therefore
structural measurements were not available.

315 A surface-based modeling approach was applied to build a three-dimensional geological model of the Pahtohavare-
Rakkurijärvi area, with the aim to facilitate the visualization and understanding of the lithological and structural framework of
the area. The horizontal extent of the model shares the boundaries with the geological map (Fig. 34) and has a vertical range

of 1000 m. The vertical range of the model was selected due to the scale of the well-known structures further north in the central Kiruna area and the open end of the structures from the shallow drillholes. A combination of explicit and implicit 3D geomodelling was utilized in Leapfrog Geo (version 2021.2.4, by Seequent). Surface structural measurements were used as implicit, primary indicators for bedding orientations and the dips were estimated from the continuation of lithological units that were traced through several drillholes. Contacts of lithological units were implemented explicitly by tracing the lithological boundaries from the geological map and drillhole sections.

4. Results

4.1 Structural analysis

The study area is located approximately 5 km south-southwest of the Kiirunavaara IOA deposit and hosts the Pahtohavare and Rakkurijärvi deposits (Fig. 3). The rocks in the study area are folded into a SE-plunging anticline which can be visualized in an aeromagnetic anomaly map of the vertical gradient of the total magnetic intensity anomaly (Fig. 3). The rocks are structurally bound to the east and southwest by shear zones trending NE-SW and NW-SE, respectively (Fig. 3). The NE-SW shear zone forms a part of the Kiruna-Naimakka deformation zone (KNDZ), and the NW-SE shear zone is hereby referred to as the Pahtohavare shear zone (PhSZ, Fig. 3). A summary of the structural mapping results on a geologic map is visualized in Fig. 4 and a full data map can be seen in the supplementary materials (S1). Outcrop exposure is approximately 5% in the field area, however from Pahtohavare, a relatively well-exposed ridgeline runs from the Pahtohavare area parallel to the axial trace of the anticline (Fig. 3) and flattens into swampy terrain towards the Rakkurijärvi area (Fig. 4). The main formations exposed include a thick horizon of basaltic pillow lavas with minor interlayers of tuffite and chemical sediments, and the Kurravaara conglomerate (Fig. 4). A densely exposed and mapped area through these units on the northern limb of the fold is summarized in Fig. 4A. The outcrop exposure on the southern limb of the fold is primarily limited to the open pit wall of the Southern Pahtohavare deposit (Fig. 4B), which consists of a series of tuffitic and gabbroic units.

The mapping results of the bedding planes collected during the 2019-2021 field campaign and from exploration of the Southeastern deposit during the 1990s are presented in a lower hemisphere, equal area stereographic projection of bedding planes (Fig. 34AC) and indicates that the geometry of the fold is non-cylindrical with a subvertical to inclined axial plane, and is moderately SE plunging ($\beta = 49/34/161/49$ fold axis). In the densely outcropping area in the northern limb of the anticline (Fig. 4A), the bedding orientations appear randomly orientated, however, they show a similar folding orientation in the stereographic projection ($\beta = 19/162$), suggesting parasitic folding occurs. Parasitic folding is also observed in the Southern Pahtohavare open pit (Fig. 5A-B) and in thin sections from drill core (Fig. 5C-D). The fold axis of one of the parasitic folds (03/090, Fig. 5B) is plotted together with the bedding and cleavage data (Fig. 4C-F) and illustrates that local deviation from the overall orientation of the large-scale fold can occur. The spatial distribution of bedding dip directions within the fold limbs are somewhat irregular, and may reflect parasitic folding, a feature that is clearly observed in outcrop at the Pahtohavare Southern open pit (Fig. 4A).

Formatted: Not Highlight

Formatted: Not Highlight

350 Foliation in the field area often occurs as a bedding sub-parallel to parallel foliation in volcanosedimentary and sedimentary units. Cleavage mapping data is plotted in Fig. 4D and show an overall similar folding pattern as the bedding, with the fold axis of the foliation occurring steeper than that of the bedding ($\beta = 76/156$). Steeply dipping foliation can be overturned. To account for possible bias from misclassification of bedding versus bedding-subparallel cleavage measurements during mapping, Figure 4C shows the combined bedding and cleavage measurements which depict illustrate a comparable folding pattern consistent with to the bedding data (Fig. 4C) geometry depicted by the bedding and the map trace of the fold axis (Fig. 3, 4). However, an important observation from this study is the presence of two distinct generations of foliation. The relationship between the two foliations has been observed in rheologically weak units such as tuffites and schists that have been parasitically folded (Fig. 5B) and also in a granitic intrusion approximately 2.5 km southwest of the PhSZ (Fig. 5E). Figure 5B shows the relationship between bedding and foliation in a parasitic fold in the Southern Pahtohavare open pit. The bedding parallel foliation is defined by biotite and scapolite and the axial plane-parallel foliation is spaced and defined by scapolite. The foliation planes have been injected into by late scapolite veins. A similar relationship has been observed in thin section (Fig. 5C-D) from a graphitic schist sample taken from drill core (full thin section micrographs can be found in S1-S2). An important observation in the Pahtohavare area is the occurrence of two distinct fabrics. A bedding-subparallel tectonic fabric is observed both in outcrop and in thin section. This thin section (unoriented) shows folded The bedding, bedding-subparallel fabric, and a spaced axial plane-parallel fabric. in thin section shows The bedding sub-parallel fabric is a pseudo-mylonitic texture containing with S-C textures (Fig. 5C) and asymmetric porphyroclasts (Fig. 5F) with consistent dextral sense of shear in both limbs of the fold and suggests non-coaxial strain. The porphyroclasts have with recrystallized strain shadows (Fig. 5G-HB-F). It is well developed in rheologically weak units such as in pyroclastic layers and graphite schists. The overprinting spaced axial plane-parallel foliation is defined by fine-grained biotite mineral alignment, as well as by veins of remobilized pyrrhotite-chalcopyrite-pyrite that have utilized S_2 deformation bands (C fabric) for injection. In certain samples, this fabric is overprinted by a spaced cleavage (Fig. 4B-D). An additional other example of two distinct fabrics is shown in an oriented thin section from a shear zone in the Southern Pahtohavare open pit by preserved foliation trails in a scapolite porphyroblast which are discordant to the foliation that wraps around it (Fig. 4I). The combined structural, outcrop, and thin section observations indicate the fold in the Pahtohavare-Rakkurijärvi area is an F_2 fold formed under non-coaxial strain, and that both S_1 and S_2 fabrics are preserved. Additionally, in the Saarijärvi area, two separate fabrics are observed affecting granitic intrusions (Fig. 4H).

375 The cleavage measurements from the Pahtohavare-Rakkurijärvi area show an overall similar folding pattern as the bedding (Fig. 3B), with the fold axis of the foliation occurring steeper than the that of the bedding ($\beta = 69/163$). To account for possible bias from misclassification of bedding versus bedding-subparallel cleavage measurements during mapping, Figure 3C shows the combined bedding and cleavage measurements which illustrate a folding pattern consistent with the geometry depicted by the bedding and the map trace of the fold.

380 Plotted together in the stereographic projections are a fold axis and axial planar fabric of a local parasitic fold from the Pahtohavare Southern open pit (purple pole and gray great circles, Fig. 3B-C), which illustrate how folding patterns can locally

Formatted: Not Highlight

Formatted: Subscript

385 deviate from the overall orientation of the fold. The parasitic fold shows evidence for bedding-subparallel foliation defined by
biotite and scapolite. Furthermore, scapolite veins mimic the orientation of the axial plane-parallel cleavage suggesting vein
injection during late tectonic processes (Druguet, 2019), consistent with brittle-plastic conditions associated to the late phase
of the Svecofennian orogeny (Andersson et al., 2020; 2021; Bauer et al., 2022). The combined structural, outcrop, and thin
section observations indicate the fold in the Pahtohavare-Rakkurijärvi area is an F_2 fold formed under non-coaxial strain, and
that both S_1 and S_2 fabrics are preserved.

390 The NE-SW trending KNDZ near the Rakkurijärvi area causes a transposition of the foliation direction into a NE-SW
orientation that quickly dissipates in outcrops away from the shear zone boundary (Fig. 4F). Tensional gashes and brittle
fracturing record tensile openings with a NW-SE orientation directly in the shear zone. The NW-SE trending PhSZ was mapped
via small-scale (10-15 cm wide) shear zones from the southern Pahtohavare open pit. One quartz-carbonate \pm pyrite \pm
chalcopyrite shear band with the orientation 80/065 indicates the shear zone is steeply dipping and a mineral lineation defined
395 by scapolite (55/162) on the foliation plane shows that oblique-reverse movement characterizes the sense of shear.

A new mine level map from the 300 m level at the Southern Pahtohavare deposit is presented in Fig. 6A. The lithological
contacts and the structures presented on the map were interpolated using vertical cross sections from 3-5 inclined drill holes
every ten meters along strike of the ore body. The geometry of the ore body indicates the mineralization is strongly structurally
controlled by undulating WNW- to NW-directed shear zones as well as by secondary brittle faults. Importantly, at the surface
400 at Southern Pahtohavare open pit, quartz-carbonate \pm pyrite \pm chalcopyrite shear bands and veins, a main ore-related mineral
assemblage for the epigenetic Pahtohavare deposits, are observed cross cutting tectonic cleavage at the Southern Pahtohavare
open pit (Fig. 4G, Fig. 54H). These veins show occur both as brittle fractures and plastic-ductile shear zones at orientations
close to parallel or at an angle to the axial plane of the fold (Fig. 4G). deformation manifested by small-scale syn-tectonic
shear bands and brittle fractures. One small-scale (10-cm-wide) quartz-carbonate \pm pyrite \pm chalcopyrite shear band mirrors
405 the orientation of the NW-SE trending shear zone (80/065) and a mineral lineation defined by scapolite (55/162) on the foliation
plane shows a moderate oblique-reverse movement. An oriented thin section from this shear zone indicates a sinistral sense of
shear and NE-side up kinematics (Fig. 4J-K). The quartz-carbonate \pm pyrite \pm chalcopyrite vein orientations from the Southern
Pahtohavare open pit are plotted in Fig. 3D with orientations either sub-parallel with or off-axis to the axial plane. Similarly,
at the Southeastern deposit (Fig. 6B), a discordant ore zone trends NNW-SSE in an off-axis orientation to the axial plane of
410 the fold. The discordant ore zone cuts the bedding in the tuffite and the gabbroic sill at a high angle and splits into lower order
structures towards the stratabound portion of the deposit. The data suggest that veining (and subsequent alteration and
mineralization) occurred syn- to post- F_2 folding in response to sinistral oblique-reverse movement and indicate that the
Pahtohavare epigenetic Cu \pm Au deposits can be structurally constrained to the late Svecofennian orogeny.

The outcrops near the Rakkurijärvi shear zone record a transposition of fabric into the NE-SW orientation of the shear zone
415 (Fig. 3E). Tensional gashes and brittle fracturing record tensile openings with a NW-SE orientation. Strain intensity abruptly
decreases with distance from the shear zone, and strain partitioning effects are common in outcrop-scale throughout the study

area (Fig. 4L). On the SE side of the shear zone, the greenstone stratigraphy occurs as a tectonically displaced unit, a feature that is also observed in the central Kiruna area (Offerberg, 1967).

4.2 Geological model

420 A 3D geological model generated based on drill hole data and the geological map (Fig. 34) visualizes the main lithological boundaries and structures for the study area (Fig. 57). The relatively shallow drill holes (down to 300 m), indicate a complex intercalation between gabbro, graphitic schist, hornblendite, chert, and greenstones composed mainly of basaltic tuff. Based on the lithological logs from the drill cores, the markers were grouped into four units: graphite schist, gabbroic sill, pillow basalts and undifferentiated greenstones. The trachyandesitic Hopukka formation, andesitic Porphyrite group, igneous granite-syenite of the PMS, and the Kurravaara conglomerate were not intersected by the selected drill holes and were traced based on the map extent to constrain the model. Faults were added based on the geological map (illustrated in red in Fig. 57) and were modeled as hard boundaries that separate fault blocks. Two perpendicular conceptual cross-sections were created based on the geological model (AA' and BB' in Fig. 57) and contain additional interpretations for an improved visualization of the crustal architecture, illustrating the SE plunging anticline and the relationship between the lithostratigraphic units. The conceptual cross sections highlight the geometry of the fold showing a curvilinear fold axis and moderate to steep plunge to the SE (Fig. 57 AA'), and the anticlinal nature with a subvertical axial plane which trends subparallel to the NW-SE PhSZ shear zone is seen in Figure 5B (Fig. 7B BB'). Furthermore, it illustrates the interplay between the major shear zones and secondary fault structures that show minimal offset but are interpreted to have formed as a result of brittle-plastic noncoaxial strain between the two conjoining shear zones. The NW-SE oriented shear zone PhSZ truncates the southwestern limb of the Pahtohavare fold and probably played an important role in controlling the shape of the fold during the deformational events.

5. Discussion

Clarifying the degree-timing of Cu-Au mineralization associated and the tectonic regime during emplacement to each stage (early and late) of the Sveco-Karelian orogeny in Norrbotten is critical for understanding the mineral systems and the relationships between IOA and IOCG deposits in Norrbotten. However, the overprinting deformation, metamorphic sm, magmatism magmatic, and alteration events associated to the Sveco-Karelian orogeny complicate interpretation of vectors to ore and the identification of ingredients of the different mineral systems. Some Cu-Au mineralization in Norrbotten has been linked to the early Sveco-Karelian orogeny (e.g. Aitik porphyry Cu (Au-Ag-Mo) deposit, cf. Fig. 1, Rakkurijärvi IOCG; Wanhainen et al., 2012; Smith et al., 2007), but a significant contribution of Cu-Au occurs as late-orogenic overprints (e.g. IOCG-overprint at Aitik and the Nautanen deformation zone as well as at the Malmberget and Gruvberget IOA deposits, Fig. 1; Wanhainen et al., 2012; Martinsson et al., 2016; Bauer et al. 2018; Bauer et al., 2022). Therefore, assessing energy drivers (e.g. magmatism, deformation etc.), fluid and metal sources, transport pathways, and traps (Wyborn et al., 1994) by framing them within the tectonic framework is useful for unraveling complicated and overprinted relationships. Bauer et al. (2018;

2022) use structural constraints on alteration and mineralization indicating Cu-Au mineralization in the Nautanen deformation zone and the Malmberget IOA deposit are hosted in late orogenic structures, and they suggest that either a late mineralization with new metal input occurred, or that tectonically late structures acted as traps for remobilized metals. The question of which mineralized deposits are associated to each tectonic phase of the Svecokarelian orogeny (early or late) and whether these represent unique mineralization events remains an important factor in understanding what genetic connection IOA and IOCG deposits share genetic relationships in northern Norrbotten. Below, the structural context and relative timing of the Pahtohavare epigenetic deposits are discussed and temporally placed. Kiruna mining district ore forming processes are temporally placed within the within the context of the tectonic framework, and Additionally, the structural setting for transport pathways and traps of the mineral systems of the Kiruna mining district are discussed.

5.1 Structural context and Timing of ore forming processes for the Pahtohavare epigenetic deposits

Structural analysis of the Pahtohavare-Rakkurijärvi area gives critical insight into the timing of ore formation for the epigenetic Pahtohavare Cu ± Au deposits. The structural characterization of the northern Norrbotten ore province defines two major periods of fabric development during the tectonic evolution Svecokarelian orogeny. Regionally, S₁ reflects an inferred NE-SW crustal shortening which formed a regionally distributed and penetrative, yet heterogeneously developed fabric (Bergman et al., 2001, Grigull et al., 2018, Bauer et al., 2018, Andersson et al., 2020, Bauer et al., 2022). S₂ records an inferred E-W crustal shortening forming a spaced fabric (Luth et al., 2018b, Grigull et al., 2018, Bauer et al., 2018, 2022, Andersson et al., 2020, 2021). The structural results from this study show A two distinct fabrics are preserved similar structural pattern is observed in the bedrock Rhyacian greenstones and lower Orosirian rocks in the Pahtohavare-Rakkurijärvi area southern Kiruna district. An early S₁ fabric occurs bedding-subparallel in volcanosedimentary and sedimentary rocks and is interpreted to be tectonically formed from non-coaxial strain based on microstructural observations of mylonitic textures and foliation is best observed in rheologically, relatively weak rocks and asymmetric sigmoidal clasts with recrystallized pressure shadows (Fig. 5C, F, G-H). Additionally, preserved foliation trails in a scapolite porphyroblast taken from the Southern Pahtohavare open pit shows an early tectonic fabric is preserved (Fig. 5I), indicate tectonic non-coaxial strain occurred during formation. The pressure shadows exclude that the fabric formed from compaction foliation along bedding, though the presence of compaction foliation in the shallower Orosirian part of the stratigraphy (Andersson et al., 2021) suggests the tectonic fabric probably overprinted (or occurred simultaneously to) a compaction fabric in the Rhyacian and lower Orosirian rocks. The bedding-subparallel foliation is here interpreted as S₁. A late S₂ fabric is observed occurring axial plane-parallel to folded bedding + S₁ foliation (Fig. 5C, S2-S3). The fabric is spaced, suggesting brittle-plastic conditions which agrees with the described nature of the late Svecokarelian deformation event (Luth et al., 2018b, Grigull et al., 2018, Andersson et al., 2020, Bauer et al., 2022). Despite two fabrics being identified microstructurally, field evidence unfortunately provided few clear outcrops showing the relationship between the two foliations. However, it is observed in parasitic folding from Pahtohavare Southern open pit (Fig. 5A-B) which also shows bedding subparallel foliation and spaced axial plane-parallel S₂ foliation. The foliation planes portrayed in the stereographic projections (Fig. 4D) therefore, were not divided into early versus late generations owing to the

Formatted: Subscript

Formatted: Subscript

Formatted: Subscript

Formatted: Subscript

lack of field relationships. However, the summary of all the cleavage data (Fig. 4D) maintains a relatively consistent fold pattern to the bedding. We presume the S_2 foliation present in the dataset trends subparallel with the fold axis of the fold in the Pahtohavare area.

485 The bedding data (Fig. 4C) agrees with the first order map trace of the fold observed in the aeromagnetic anomaly map (Fig. 3). Furthermore, the data show that the fold is noncylindrical and suggests that the plunge of the fold can vary between steep to shallow. This is observed from the data plotted from the northern limb (Fig. 4A) which shows a moderately shallow dip, compared to the overall plunge of the fold from the bedding data which is steeper (Fig. 4C). Additionally, the parasitic fold measured from the Southern Pahtohavare open pit (Fig. 5B), has a near horizontal fold axis (03/090). Therefore, our conceptual interpretation of this feature (Fig. 7A) shows a fold plunging to the SE that has a curvilinear fold axis. Parasitic folding is 490 observed both in drill core (Fig. 5C), outcrop (Fig. 5A-B), and can be deduced from the mapping measurements in the field (Fig. 4A). While the single measurement of the fold axis of the parasitic fold deviates from the main orientation of the fold in the area (Fig. 4C, 5B), this could be explained by deflection or transposition during folding and/or shearing. Further evidence that the parasitic folds are associated to the SE plunging anticline is the apparent random orientations of bedding planes in the northern limb, that when plotted into a stereographic projection shows a similar fold axis plunge direction, arguing for a coaxial relationship (Fig. 4A). Together, the bedding and cleavage results strongly indicate that the anticline in the Pahtohavare-Rakkurjärvi area is an F_2 fold formed during the late Svecokarelian orogeny.

495 Kinematic data on the PhSZ has not previously been described with structural data. The results in this study show that the shear zone is steeply dipping to the NE (80/065) based on data from local small-scale (10-20 cm wide) shear zones in the Southern open pit. In the shear bands, quartz-ferrodolomite-calcite-pyrite-chalcopyrite mineral assemblages are boudinaged and infiltrate along folded bedding planes which reflect plastic behavior during syn-tectonic emplacement, likely coeval to the 500 folding. A scapolite mineral lineation on a foliation plane within the shear zone indicates movement with an orientation 55/162. To form the anticlinal fold from E-W crustal shortening during the late Svecokarelian requires that the movement along the shear zone was dominantly reverse with a minor sinistral component as opposed to a normal-dextral movement.

505 The Pahtohavare Southern and Southeastern deposits are both strongly structurally controlled (Fig. 6). A WNW- to NW-oriented structure shears the Southern deposit (Fig. 6A) forming steep shear contacts between the ore and the host rocks. Similarly, at the Southeastern deposit, a subvertical NNW-oriented shear structure controls the discordant ore zone which cuts the hosting mafic sill and the bedding in the tuffite at a high angle (Fig. 6B). The orientation of these features form either an axial plane-parallel orientation to the Pahtohavare fold (Southern) or an acute angle to the PhSZ (Southeastern) and likely represent secondary brittle-ductile faults formed in response to reverse oblique shearing along the shear zone during the late 510 Svecokarelian orogeny. The orientations of the quartz-carbonate veins from the Southern Pahtohavare open pit show either a N-S to NNW- or an E-W orientation (Fig. 4G) which support that lower order structures play a role in the mineralization. The quartz-carbonate veins also cross cut tectonic foliation (Fig. 5J) in the Southern Pahtohavare open pit indicating a late Svecokarelian orogenic timing for emplacement.

Formatted: Normal, No bullets or numbering

Formatted: Subscript

In the absence of a regional tectonic framework and geochronological constraints, the timing of the epigenetic Pahtohavare deposits was unknown but suggested to be of similar age as the Rakkurijärvi IOCG deposit, for which radiometric age data (Re-Os molybdenite, U-Pb LA-ICP-MS allanite, U-Pb TIMS rutile) indicate formation at ca. 1.86 Ga (Smith et al., 2007, 2009; Martinsson et al., 2016). However, the results of this structural investigation and the designation of the Pahtohavare fold as F_2 allows the Pahtohavare epigenetic deposits to be assigned to the late Sveco-Karelian mineral system, which in Kiruna is constrained by syn-tectonic titanite data at ca. 1.81-1.79 Ga (Andersson et al. 2022). Furthermore, this illustrates that brittle-ductile, non-coaxial shear zones and resultant S_2 and lower order structures associated to the E-W-oriented late orogenic deformation served as pathways for ore fluids. In the Pahtohavare area, traps for the mineral system likely occur where these pathways intersected favorable reducing horizons of graphitic schist, which has been shown to be an important lithological trap for the ore (Martinsson et al., 1997a). The structural results from this study are the first to show a late-Sveco-Karelian timing for Cu ± Au mineralization in the Kiruna mining district. Given the subparallel orientation to bedding of the tectonic S_1 and the correlating folding pattern of the bedding and cleavage measurements (Fig. 3B-C), the anticline in the Pahtohavare-Rakkurijärvi area can be constrained as an F_2 fold resulting from late Sveco-Karelian orogenic deformation. In thin section, the S_2 foliation is observed occurring as spaced cleavage and axial planar to parasitic F_2 folds (Fig. 4B-C), a characteristic also seen regionally (Luth et al., 2018b, Grigull et al., 2018, Andersson et al., 2020, Bauer et al., 2022). Both S_1 and S_2 cleavage data are likely represented in Figure 3B-C, however, without observations of cross-cutting relationships in the field, the separate generations were not divided on the stereographic projection. However, S_2 cleavage is presumed to trend subparallel with the axial plane of the F_2 fold.

Importantly, in the Southern Pahtohavare open pit, ore-related quartz-carbonate ± pyrite ± chalcopyrite veins and narrow (10-20 cm wide) shear bands are observed cutting an earlier tectonic foliation (Fig. 4I). In the shear bands, quartz-ferrodolomite-calcite-pyrite-chalcopyrite mineral assemblages are boudinaged and infiltrate along folded bedding planes which reflect plastic behavior during syn-tectonic emplacement, likely coeval to the folding. However, the orientation of the veins varies from axial plane parallel to orientations at an angle to the axial plane (Fig. 3D), utilizing tensional fractures during shearing and folding which comparatively indicates brittle-plastic conditions. Previous documentation of Southern and Southeastern Pahtohavare has described the deposits are structurally controlled especially in structures at an angle to the fold hinge (Martinsson et al., 1997a). In the absence of a regional tectonic framework and geochronological constraints, the timing of the epigenetic Pahtohavare deposits was unknown but suggested to be of similar age as the Rakkurijärvi IOCG deposit, for which radiometric age data (Re-Os molybdenite, U-Pb LA-ICP-MS allanite, U-Pb TIMS rutile) indicate formation at ca. 1.86 Ga (Smith et al., 2007, 2009; Martinsson et al., 2016). However, the results of the structural investigation and the designation of the Pahtohavare fold as F_2 allows the Pahtohavare epigenetic deposits to be assigned to the late Sveco-Karelian mineral system, which in Kiruna is constrained by syn-tectonic titanite data at ca. 1.81-1.79 Ga (Andersson et al. 2022). Furthermore, this illustrates that brittle-ductile, non-coaxial shear zones and resultant S_2 structures associated to the E-W-oriented late orogenic deformation served as pathways for ore fluids. In the Pahtohavare area, traps for the mineral system likely occur where these pathways intersected favorable reducing horizons of graphitic schist, which has been shown to be an important lithological trap for the ore

(Martinsson et al., 1997a). The structural results from this study are the first to show a late-Svecofennian timing for Cu ± Au mineralization in the Kiruna mining district.

550 5.2 Structural framework in Kiruna

A conflicting result from this study that complicates the interpretation of how the regional tectonic evolution is expressed in the Kiruna mining district is the preserved S_0 foliation in the Rhyacian greenstone rocks (Kiruna greenstone group) and lower Orosirian rocks (Kurravaara conglomerate) which is absent or masked in the overlying Orosirian rocks (Andersson et al., 2021). The structural framework of the Kiruna mining district presents ambiguities in context of the regional tectonic evolution.

555 While an S_1 fabric is observed regionally (Bergman et al., 2001, Grigull et al., 2018, Bauer et al., 2018, Andersson et al., 2020, Bauer et al., 2022), in the Kiruna mining district it is absent or masked in the structural data obtained from the Orosirian part of the stratigraphy (Andersson et al., 2021). Subsequently, Andersson et al. (2021) suggested the lack of an S_0 fabric in the central Kiruna area was suggested to indicate the rocks were at represents a higher crustal level that was too shallow to have did not experienced plastic deformation during the early orogenic phase. Furthermore, to the west and southeast of Kiruna structural evidence shows that blocks of lower crustal levels (and subsequently higher metamorphic grades) were uplifted with reverse west-side-up kinematics along steep west-dipping structures southeast and west of Kiruna (Lynch et al., 2015; Bergman et al., 2001; Andersson et al., 2020) and with to the east and northeast, reverse east-side-up kinematics to the east and northeast occur along east-dipping structures (Luth et al., 2018b, Andersson et al., 2021). Other structural investigations have noted that the Kiruna area records fewer folding phases compared to the regions to the north and east (Vollmer et al., 1984; Grigull et al., 2018; Luth et al., 2018b).

565 A bedding-parallel S_0 compaction fabric is described for the Orosirian sequence in the central Kiruna area, however, The results of the current study document the presence of an S_1 tectonic fabric in the bedrock that underlies the Orosirian sequence (Kiruna greenstone group and Kurravaara conglomerate) around Pahtohavare, Rakkurijärvi, and Saarijärvi (Fig. 2-3). In addition to the pressure shadows on porphyroclasts and mylonitic the mylonitic bedding-subparallel fabric observed in thin section (Fig. 4B-F5C-D), the the presence an early- S_1 foliation trails fabric in a scapolite porphyroblast (Fig. 4G5J), and of the two generations of tectonic fabric in granitic intrusions in the southern part of the district (Fig. 4H5E) excludes that the foliation in these areas is a result offrom compaction alone. Evidence of S_1 (or S_0/S_1) and S_2 fabrics is also noted in a previous mapping campaign in the Saarijärvi area (Martinsson et al., 1993). The current study indicates that the deeper stratigraphy belonging to the Rhyacian and lower Orosirian rocks in the southern Kiruna mining district were affected by a tectonic foliation forming event while the higher Orosirian rocks in the central Kiruna were not. Two possible explanations for this discrepancy are that the S_0 fabric developed heterogeneously in response to shearing and/or to an elevated geothermal gradient. Relatively localized S_1 shearing foliation could account for the locally and heterogeneously developed tectonic fabric found in the greenstones sequence (e.g. graphite schists, pyroclastic tuffs, mafic sills, e.g. Fig. 4B-F5B-C, 4I5J). However, the two generations of foliation in competent rocks (e.g. granitic outcrops in the southern part of the district, Fig. 4H) calls for ductile deformation could also have occurred due to possibly explained by a locally elevated geothermal gradient in this area. Logan

Formatted: Subscript

Formatted: Subscript

Formatted: Subscript

Formatted: Subscript

Formatted: Not Highlight

et al. (2022) recently conducted U-Pb zircon geochronology on several intrusions in the southern part of the district that showed a dominantly early Svecofennian timing for the magmatism. The abundant magmatism would have resulted in increased fluid circulation and may have facilitated the heterogeneous formation of a ductile S₁ fabric. Extensive hydrothermal fluid flow driven by abundant igneous activity has been postulated as an explanation for the regional style Na-metasomatism (e.g. scapolite and albite), which is also restricted to large-scale shear zones (Frietsch et al., 1997; Bergman et al., 2001). In the central Kiruna area the regional-style scapolite alteration occurs more rarely (Bergman et al., 2001, Martinsson 2004), and the Na-Ca (+ Fe ± Cl) and alkali alteration styles recorded are spatially associated to local IOA deposits (Martinsson, 2015; Martinsson et al., 2016).

A conceptual framework of the structural evolution of the Kiruna area is proposed in [Figure 68](#) which synthesizes the structural results presented in this paper with those produced by Andersson et al. (2021), and is also based on previous structural mapping from the Kiruna area (Wright, 1988; Martinsson et al., 1993; Grigg et al., 2018) as well as the Geological Survey of Sweden's magnetic anomaly map of the district ([Fig. 3](#); Bergman et al. 2001). This framework is offered as a working model and can be subject to modification with future work in the district. The NW-SE-trending [PhSZ shear zone](#) to the southwest of the fold in the Pahtohavare-Rakkurijärvi area, ~~here referred to as the Pahtohavare shear zone,~~ is interpreted to be a reactivated early normal fault structure. This structure formed during the back arc extension of the early Svecofennian orogeny ([Fig. 68A](#)), or possibly even earlier during the Rhyacian rifting. Upon the early NE-SW oriented crustal shortening at ca. 1.87 Ga ([Fig. 68B](#)), the structure reactivated with reverse kinematics and an early tectonic S₁ fabric was heterogeneously developed, possibly forming as a shear foliation and/or as a result of a locally elevated geothermal gradient. At the same time, the NE-SW to N-S [KNDZ structure](#) that runs adjacent to the Rakkurijärvi deposit and through central Kiruna ([Fig. 2-34](#)), would have responded with oblique reverse shearing ([Fig. 68B](#)) and offered conduits along which ore fluids could transport. During the E-W brittle-plastic crustal shortening of the late Svecofennian orogeny, extensive reactivation of fault systems occurred in the Kiruna mining district ([Fig. 68C](#)). Basin inversion manifested from the crustal shortening (Andersson et al., 2021) and strong strain partitioning occurred, forming high strain fabrics along shear zones, and spaced- to heterogeneously-developed fabric outside of these zones. Conjugate faulting subparallel to the E-W shortening direction occurred in response to the stress direction ([Fig. 8C](#)). The ~~Pahtohavare shear zone~~ [PhSZ](#) responded with ~~sinistral~~ [sinistral](#) reverse-oblique ([sinistral](#)) kinematics causing vertical extrusion of the rocks and non-cylindrical anticlinal folding ([Fig. 7, 9](#)). This juxtaposed the older Rhyacian volcanic rocks to the northeast with younger Orosirian volcanic rocks on the southwest ([Fig. 34, 79](#)). During this time the brittle-ductile strain created tensional structures for ore fluids to propagate through in the Pahtohavare area. Finally, at ca. <1.79 Ga (cf. Andersson et al., 2022), a N-S oriented crustal shortening led to gentle refolding (Andersson et al., 2021) and minor reactivation of preexisting fault structures ([Fig 86D](#)).

Formatted: Not Highlight

5.3 Implications for the Kiruna mining district mineral systems and relationships between IOA and IOCG mineralization

This study shows that multiple mineralization events in the Kiruna mining district can be linked to specific phases of the tectonic evolution. Using the proposed structural framework presented in [Figure 68](#), the timing of mineralization within a structural context can be synthesized. The earliest mineralization known in the district (e.g. Viscaria and Eastern Pahtohavare, [Fig. 2](#)) has been suggested to have occurred syngenetically during deposition of the Kiruna greenstone group around ca. 2.1 Ga from Rhyacian rifting (Martinsson et al., 1997a, b). Following this mineralization and rifting period, during the Orosirian back arc extension and basin development in the district, the development of syn-volcanic normal and transtensional faults ([Fig. 86A](#)) occurred around 1889 ± 26 Ma (Andersson et al., 2022), shown by in situ U-Pb (LA-ICP-MS) dating of titanite in a hydrothermally altered damage zone to a fault system associated with the Luossavaara IOA deposit. Such a timing is coeval with volcanism in the district as well as the accepted age for the IOA formation (1888 ± 6 , U-Pb ICP-MS titanite; 1874 ± 7 Ma and 1877 ± 4 Ma, U-Pb SIMS zircon; 1878 ± 4 Ma, U-Pb TIMS titanite; Romer et al., 1994, Westhues et al., 2016, Martinsson et al., 2016). It was therefore suggested that normal faulting in an extensional regime may have played an important role for the emplacement of the IOA ore (Andersson et al., 2022). Conversely, following the onset of crustal shortening ([Fig. 86B](#)), the Rakkurijärvi IOCG deposit formed and is described to be related to the NE-SW shear zone ([KNDZ](#)) adjacent to the deposit (Smith et al., 2007), implying that the faulting activity was active around ore formation at ca. 1.86 Ga (Smith et al., 2007, 2009, Martinsson et al., 2016). Such a context supports that IOA and IOCG deposits may form within 20 Myr of each other as indicated in other classic IOCG-IOA terrains (e.g. the Chilean iron belt; c.f. Skirrow 2021 and references therein). It is possible that IOA and IOCG deposits share some mineral system ingredients, however, in Kiruna distinct tectonic regimes separate the formation of IOA and IOCG deposits respectively ([Fig. 86A-C](#)).

The establishment of a late orogenic timing for the epigenetic Pahtohavare Cu \pm Au deposits indicates that a time gap of ca. 80 Myr or more exists between the younger episode of Cu \pm Au mineralization and the IOA emplacement in the Kiruna mining district. The indicated time-gap introduces important implications for the current debates about IOA and IOCG genetic continuums (c.f. Reich et al., 2016; Corriveau et al., 2016; Barra et al., 2017; Simon et al., 2018; del Real et al., 2021) as the later Cu \pm Au event in Norrbotten lacks clear temporal associations to IOA deposits; this is in line with the mineralization in the Cloncurry district in Australia where IOCG-style deposits occur without Kiruna-type IOA deposits (cf. Groves et al., 2010; Reich et al., 2022). Furthermore, in the Gällivare area, approximately 70 km southeast of Kiruna (cf. [Fig. 1](#)), two distinct mineralizing periods related to different phases of the tectonic evolution are also described. The Malmberget IOA deposit is considered to have formed during the early orogenic phase (ca. 1.89-1.88 Ga), constrained by the age of the host rocks (Sarlus et al., 2020) and from structural analysis showing the iron ore was affected by two deformation events (Bergman et al., 2001, Bauer et al., 2018). Late IOCG-style mineralization is suggested to have overprinted the area around 1.80 Ga at Aitik (Wanhainen et al., 2012) as well as in the Nautanen deformation zone where mineralization is also situated in late orogenic structures (Bauer et al., 2022). From a mineral systems perspective, multiply-reactivated structures (e.g. [Fig. 68](#)) may play an important role for fluid and transport pathways even if IOA and IOCG-style mineralization can be separated in time and by

645 tectonic regimes. For example, the N-S to NE-SW trending structure adjacent to the shear zone-controlled Rakkurijärvi IOCG
deposit (Fig. 2, ~~3-4~~) can be constrained by radiometric age determinations (ca. 1.86 Ga; Smith et al., 2007; 2009; Martinsson
et al., 2016), but has also been shown by structural analysis to be active during the late Svecokarelian orogeny (ca. 1.81-1.79
Ga; Andersson et al., 2021, 2022). Furthermore, U-Pb (SC-ICP-MS) ages from monazite in hydrothermal calcite found within
650 the same shear zone in central Kiruna show that the structure was again active at ca. 1.78-1.76 Ga (Lauri et al., 2022). The
point that these reactivated transport pathways facilitated overprinting alterations and mineralization emphasizes the
importance of ~~utilizing and incorporating the~~ tectonic framework ~~for assessing into the assessment of~~ these complex mineral
systems.

6. Conclusion

The northern Norrbotten ore province has a complex tectonic evolution and mineralization history and requires that mineral
655 systems assessments be made utilizing a regional tectonic framework. The Pahtohavare-Rakkurijärvi area in the Southern
Kiruna mining district hosts syngenetic and epigenetic Cu ± Au and IOCG mineral occurrences which have not been
~~structurally~~ contextualized within the ~~structural-tectonic~~ evolution of the region. In the Pahtohavare-Rakkurijärvi area, the
Rhyacian to lower Orosirian volcanic, volcanoclastic, and sedimentary bedrock is anticlinally folded and bound by two shear
zones trending NW-SE on the southwestern limb, and NE-SW to the east. New structural data show the fold is noncylindrical,
660 has a subvertical to steeply inclined axial plane, with a fold axis plunging to the SE, in agreement with previous work. Bedding
sub-parallel foliation shows an accordant folding pattern and structural analysis from thin section shows the foliation is
mylonitic and has porphyroclasts with pressure shadows, supporting ~~it is a tectonic fabric~~ a tectonic origin for the S₁ fabric.
The data constrains the fold in the Pahtohavare-Rakkurijärvi area as F₂ with folded S₁ foliation and axial plane-parallel S₂
foliation developed. Importantly, ~~the epigenetic Cu ± Au Pahtohavare deposits are strongly structurally-controlled, and~~ quartz-
665 carbonate-sulfide vein generations ~~related to the epigenetic Cu ± Au Pahtohavare deposits~~ are observed cutting foliation and
trending axial plane parallel and at an angle to the F₂ Pahtohavare fold axis trace, structurally constraining the deposits to the
late orogenic phase of the Svecokarelian orogeny. These results mark the first time a deposit in the Kiruna mining district has
been linked to the late phase of the orogeny. The shear zones binding the fold in the Pahtohavare-Rakkurijärvi area are
interpreted to be reactivated early structures and oblique reverse kinematics are proposed for the NW-SE shear zone to explain
670 the geometry of the fold in response to E-W crustal shortening. A time gap of ~80 Myr between the formation of the
Kiirunavaara IOA deposit and the formation of the Pahtohavare epigenetic Cu ± Au deposits holds important implications
about the timing of iron oxide (apatite) and copper-gold precipitation in Kiruna, showing at least two distinct mineralizing
periods can be constrained to different phases of the tectonic evolution.

Author Contributions

675 L.L. conducted the geological mapping, processed the structural data, sampled, and conducted thin section petrography,
visualized the results, wrote the original manuscript, and reviewed and edited the final manuscript. E.C.-V. made the 3D
geologic model from drill logs, visualized the results, wrote sections of the original manuscript, and edited the final manuscript.
J.B.H.A. assisted with field work and structural interpretations, [visualized the mine maps](#), and edited the final manuscript.
O.M. [conducted geologic mapping, drew the original mine maps](#), assisted with structural interpretations, and edited the final
680 manuscript. T.E.B. secured funding, supervised, assisted with field work and structural interpretations, visualized the results,
and edited the final manuscript.

Competing Interests

The authors declare that they have no conflict of interest.

Acknowledgments

685 This work is part of the European Union's Horizon 2020 project "New Exploration Technologies – NEXT" (Grant Agreement
No. 776804). Lovisagravan AB and Critical Metals Scandinavia AB are thanked for providing access to open pits. Petroleum
Experts Ltd. is thanked for donating the MOVE 2017 software. The staff at the Geological Survey of Sweden is thanked for
their help and collaboration during sampling at the National Drill Core Archive in Malå, Sweden. [Thorkild Rasmussen is
thanked for reducing the aeromagnetic anomaly data. The constructive input from Pietari Skyttä and Giovanni Musumeci
690 greatly improved the manuscript, and they are thanked for their reviews.](#)

References

- [Andersson, J. B. H., Bauer, T. E., and Lynch, E. P.: Evolution of structures and hydrothermal alteration in a
Palaeoproterozoic supracrustal belt: Constraining paired deformation–fluid flow events in an Fe and Cu–Au prospective
terrain in northern Sweden, *Solid Earth*, 11, 547–578, <https://doi.org/10.5194/se-11-547-2020>, 2020.](#)
- 695 [Andersson, J. B. H., Bauer, T. E., and Martinsson, O.: Structural Evolution of the Central Kiruna Area, Northern Norrbotten,
Sweden: Implications on the Geologic Setting Generating Iron Oxide-Apatite and Epigenetic Iron and Copper Sulfides, *Econ
Geol*, 116, 1981–2009, <https://doi.org/10.5382/econgeo.4844>, 2021.](#)
- [Andersson, J. B. H., Logan, L., Martinsson, O., Chew, D., Kooijman, E., Kielman-Schmitt, M., Kampmann, T. C., and
Bauer, T. E.: U-Pb zircon-titanite-apatite age constraints on basin development and basin inversion in the Kiruna mining
700 district, Sweden, *Precambrian Research*, 372, 106613, <https://doi.org/10.1016/j.precamres.2022.106613>, 2022.](#)
- [BABEL Working Group: Evidence for early Proterozoic plate tectonics from seismic reflection profiles in the Baltic shield,
Nature, 348, 34–38, <https://doi.org/10.1038/348034a0>, 1990.](#)

- Barra, F., Reich, M., Selby, D., Rojas, P., Simon, A., Salazar, E., and Palma, G.: Unraveling the origin of the Andean IOCG clan: A Re-Os isotope approach, *Ore Geol. Rev.*, 81, 62–78, <https://doi.org/10.1016/j.oregeorev.2016.10.016>, 2017.
- 705 Barton, M. D.: Iron Oxide(-Cu-Au-REE-P-Ag-U-Co) Systems, in: *Treatise on Geochemistry*, Elsevier, 515–541, <https://doi.org/10.1016/B978-0-08-095975-7.01123-2>, 2014.
- Bauer, T. E. and Andersson, J. B. H.: Structural controls on Cu-Au mineralization in the Svappavaara area, northern Sweden: The northern continuation of the Nautanen IOCG-system (paper II), in: *Paleoproterozoic deformation in the Kiruna-Gällivare area in northern Norrbotten, Sweden: Setting, character, age, and control of iron oxide-apatite deposits* (PhD Thesis), edited by: Andersson, J. B. H., Luleå University of Technology, Luleå, Sweden, 1–15, 2021.
- 710 Bauer, T. E., Skyttä, P., Allen, R. L., and Weihed, P.: Syn-extensional faulting controlling structural inversion – Insights from the Palaeoproterozoic Vargfors syncline, Skellefte mining district, Sweden, *Precambrian Res.*, 191, 166–183, <https://doi.org/10.1016/j.precamres.2011.09.014>, 2011.
- 715 Bauer, T. E., Andersson, J. B. H., Sarlus, Z., Lund, C., and Kearney, T.: Structural Controls on the Setting, Shape, and Hydrothermal Alteration of the Malmberget Iron Oxide-Apatite Deposit, Northern Sweden, *Econ Geol.*, 113, 377–395, <https://doi.org/10.5382/econgeo.2018.4554>, 2018.
- Bauer, T. E., Lynch, E. P., Sarlus, Z., Drejning-Carroll, D., Martinsson, O., Metzger, N., and Wanhainen, C.: Structural Controls on Iron Oxide Copper-Gold Mineralization and Related Alteration in a Paleoproterozoic Supracrustal Belt: Insights from the Nautanen Deformation Zone and Surroundings, Northern Sweden, *Economic Geology*, 117, 327–359, <https://doi.org/10.5382/econgeo.4862>, 2022.
- 720 Bergman, S.: *Geology of the Northern Norrbotten ore province, northern Sweden*, Geological Survey of Sweden, 2018.
- Bergman, S. and Weihed, P.: Chapter 3 Archean (>2.6 Ga) and Paleoproterozoic (2.5–1.8 Ga), pre- and syn-orogenic magmatism, sedimentation and mineralization in the Norrbotten and Överkalix lithotectonic units, Svecokarelian orogen, *Geological Society, London, Memoirs*, 50, 27–81, <https://doi.org/10.1144/M50-2016-29>, 2020.
- 725 Bergman, S., Kübler, L., and Martinsson, O.: Description of regional geological and geophysical maps of northern Norrbotten County (east of the Caledonian orogen), *Sveriges geologiska undersökning*, Uppsala, 110 pp., 2001.
- Bergman, S., Billström, K., Persson, P.-O., Skiöld, T., and Evins, P.: U-Pb age evidence for repeated Palaeoproterozoic metamorphism and deformation near the Pajala shear zone in the northern Fennoscandian shield, *GFF*, 128, 7–20, <https://doi.org/10.1080/11035890601281007>, 2006.
- 730 Bingen, B., Solli, A., Viola, G., Torgersen, E., Sandstad, J. S., Whitehouse, M. J., Röhr, T. S., Ganerød, M., and Nasuti, A.: Geochronology of the Palaeoproterozoic Kautokeino Greenstone Belt, Finnmark, Norway: Tectonic implications in a Fennoscandia context, *NJG*, 95, 365–396, <https://doi.org/10.17850/njg95-3-09>, 2015.
- Blomgren, H.: *U-Pb Dating of Monazites from the Kiirunavaara and Rektorn Ore Deposits*, Master of Science, University of Gothenburg, Gothenburg, 41 pp., 2015.
- 735 Cliff, R. A. and Rickard, D.: Isotope systematics of the Kiruna magnetite ores, Sweden: Part 2. Evidence for a secondary event 400 m.y. after ore formation, *Econ Geol.*, 87, 1121–1129, <https://doi.org/10.2113/gsecongeo.87.4.1121>, 1992.
- Cliff, R. A., Rickard, D., and Blake, K.: Isotope systematics of the Kiruna magnetite ores, Sweden: Part 1. Age of the ore, *Econ Geol.*, 85, 1770–1776, <https://doi.org/10.2113/gsecongeo.85.8.1770>, 1990.

- 740 Corriveau, L., Montreuil, J.-F., and Potter, E. G.: Alteration Facies Linkages Among Iron Oxide Copper-Gold, Iron Oxide-Apatite, and Affiliated Deposits in the Great Bear Magmatic Zone, Northwest Territories, Canada, *Econ Geol.* 111, 2045–2072, <https://doi.org/10.2113/econgeo.111.8.2045>, 2016.
- Day, W. C., Slack, J. F., Ayuso, R. A., and Seeger, C. M.: Regional Geologic and Petrologic Framework for Iron Oxide ± Apatite ± Rare Earth Element and Iron Oxide Copper-Gold Deposits of the Mesoproterozoic St. Francois Mountains Terrane, Southeast Missouri, USA, *Economic Geology*, 111, 1825–1858, <https://doi.org/10.2113/econgeo.111.8.1825>, 2016.
- 745 Druguet, E.: Deciphering the presence of axial-planar veins in tectonites, *Geoscience Frontiers*, 10, 2101–2115, <https://doi.org/10.1016/j.gsf.2019.02.005>, 2019.
- Frietsch, R.: Petrology of the Kurravaara Area Northeast of Kiruna northern Sweden, *Sveriges Geologiska Undersökning*, Uppsala, 1979.
- 750 Frietsch, R., Tuisku, P., Martinsson, O., and Perdahl, J.-A.: Early Proterozoic Cu-(Au) and Fe ore deposits associated with regional Na-Cl metasomatism in northern Fennoscandia, *Ore Geol. Rev.*, 12, 1–34, [https://doi.org/10.1016/S0169-1368\(96\)00013-3](https://doi.org/10.1016/S0169-1368(96)00013-3), 1997.
- Geijer, P.: Geology of the Kiruna District 2: Igneous rocks and iron ores of Kiirunavaara, Luossavaara and Tuolluvaara, Stockholm, 1910.
- Geijer, P.: Recent Developments at Kiruna, *Sveriges Geologiska Undersökning*, 22 pp., 1919.
- 755 Grigull, S., Berggren, R., Jönberger, J., Jönsson, C., Hellström, S., and Luth, S.: Folding observed in Paleoproterozoic supracrustal rocks in northern Sweden, *Geological Survey of Sweden*, 2018.
- Groves, D. I., Bierlein, F. P., Meinert, L. D., and Hitzman, M. W.: Iron Oxide Copper-Gold (IOCG) Deposits through Earth History: Implications for Origin, Lithospheric Setting, and Distinction from Other Epigenetic Iron Oxide Deposits, *Econ Geol.* 105, 641–654, <https://doi.org/10.2113/gsecongeo.105.3.641>, 2010.
- 760 Hietanen, A.: Generation of potassium-poor magmas in the northern Sierra Nevada and the Svecofennian of Finland, *J Res US Geol Surv.* 3, 631–645, 1975.
- Högdahl, K., Andersson, U. B., and Eklund, O. (Eds.): *The Transscandinavian Igneous Belt (TIB) in Sweden: a review of its character and evolution*, Geological Survey of Finland, Espoo, 125 pp., 2004.
- 765 Lahtinen, R., Korja, A., and Nironen, M.: Paleoproterozoic tectonic evolution, in: *Precambrian Geology of Finland - Key to the Evolution of the Fennoscandian Shield*, edited by: Lehtinen, M., Nurmi, P. A., and Rämö, O. T., Elsevier B.V., Amsterdam, 481–532, 2005.
- Lauri, L. S., Miles, J., Liu, X., and O'Brien, H.: Age and C-O isotopes of the hydrothermal breccias within the Kiruna-Naimakka zone, Norrbotten, Sweden, Geological Society of Sweden, 150 year anniversary meeting, Uppsala, 244–245, 2022.
- 770 Lindblom, S., Broman, C., and Martinsson, O.: Magmatic-hydrothermal fluids in the Pahtohavare Cu-Au deposit in greenstone at Kiruna, Sweden, 31, 307–318, 1996.
- Logan, L., Andersson, J. B. H., Whitehouse, M. J., Martinsson, O., and Bauer, T. E.: Energy Drive for the Kiruna Mining District Mineral System(s): Insights from U-Pb Zircon Geochronology, *Minerals*, 12, 875, <https://doi.org/10.3390/min12070875>, 2022.

- 775 Lundbohm, H. J.: Sketch of the Geology of the Kiruna district, *Geologiska Föreningen i Stockholm Förhandlingar*, 32, 751–788, <https://doi.org/10.1080/11035891009443831>, 1910.
- Luth, S., Jönsson, C., Grigull, S., Berggren, R., van Assema, B., Smoor, W., and Djuly, T.: The Pajala deformation belt in northeast Sweden: Structural geological mapping and 3D modelling around Pajala, Geological Survey of Sweden, 2018a.
- 780 Luth, S., Jönberger, J., and Grigull, S.: The Vakko and Kovo greenstone belts: Integrating structural geological mapping and geophysical modelling, Geological Survey of Sweden, 2018b.
- Lynch, E. P., Jönberger, J., Bauer, T. E., Sarlus, Z., and Martinsson, O.: Barents project 2014: Meta-volcanosedimentary rocks in the Nautanen area, Norrbotten: preliminary lithological and deformation characteristics, *Sveriges geologiska undersökning*, Uppsala, 2015.
- 785 Martinsson, O.: Tectonic Setting and Metallogeny of the Kiruna Greenstones, Doctoral Thesis, Luleå tekniska universitet, Lulea, Sweden, 162 pp., 1997.
- Martinsson, O.: Geology and Metallogeny of the Northern Norrbotten Fe-Cu-Au Province, in: *Svecofennian ore-forming environments of northern Sweden- volcanic associated Zn-Cu-Au-Ag, intrusion related Cu-Au, sediment hosted Pb-Zn, and magnetite-apatite deposits in northern Sweden*, edited by: Allen, R. L., Martinsson, O., and Weihed, P., *Society of Economic Geologists*, 131–148, 2004.
- 790 Martinsson, O.: Genesis of the Per Geijer apatite iron ores, Kiruna area, northern Sweden, SGA biennial meeting 2015, Nancy, France, 23–27, 2015.
- Martinsson, O. and Hansson, K.-E.: Apatite Iron Ores in the Kiruna Area, in: *Svecofennian ore-forming environments of northern Sweden- volcanic associated Zn-Cu-Au-Ag, intrusion related Cu-Au, sediment hosted Pb-Zn, and magnetite-apatite deposits in northern Sweden*, vol. 33, *Society of Economic Geologists*, 173–175, 2004.
- 795 Martinsson, O. and Perdahl, J.-A.: Paleoproterozoic extensional and compressional magmatism in northern Norrbotten, northern Sweden (Paper II), in: *Svecofennian volcanism in northernmost Sweden* (PhD Thesis), edited by: Perdahl, J.-A., Luleå University of Technology, Luleå, Sweden, 161, 1995.
- Martinsson, O., Perdahl, J.-A., and Bergman, J.: Greenstone and porphyry hosted ore deposits in northern Norrbotten, *Nutek*, 1993.
- 800 Martinsson, O., Hallberg, A., Söderholm, K., and Billström, K.: Pahtohavare - an epigenetic Cu-Au deposit in the Paleoproterozoic Kiruna Greenstones (Paper III), in: *Tectonic Setting and Metallogeny of the Kiruna Greenstones* (PhD Thesis), edited by: Martinsson, O., Luleå University of Technology, Luleå, Sweden, 37, 1997a.
- Martinsson, O., Hallberg, A., Broman, C., Godin-Jonasson, L., Kisiel, T., and Fallick, A. E.: Viscaria - a syngenetic exhalative Cu-deposit in the Paleoproterozoic Kiruna Greenstones (Paper II), in: *Tectonic Setting and Metallogeny of the Kiruna Greenstones* (PhD Thesis), edited by: Martinsson, O., Luleå University of Technology, Luleå, Sweden, 57, 1997b.
- 805 Martinsson, O., Vaasjoki, M., and Persson, P.-O.: U-Pb zircon ages of Archaean to Palaeoproterozoic granitoids in the Torneträsk-Råstojaure area, northern Sweden, in: *Radiometric dating results 4*, Geological Survey of Sweden, Uppsala, 70–90, 1999.
- 810 Martinsson, O., Billström, K., Broman, C., Weihed, P., and Wanhainen, C.: Metallogeny of the Northern Norrbotten Ore Province, northern Fennoscandian Shield with emphasis on IOCG and apatite-iron ore deposits, *Ore Geol. Rev.*, 78, 447–492, <https://doi.org/10.1016/j.oregeorev.2016.02.011>, 2016.

- Martinsson, O., Bergman, S., Persson, P.-O., Schöberg, H., Billström, K., and Shumlyanskyy, L.: Stratigraphy and ages of Palaeoproterozoic metavolcanic and metasedimentary rocks at Kävmäjärvi, northern Sweden. Geological Survey of Sweden, 2018.
- 815 Mellqvist, C.: The Archaean–Proterozoic Palaeoboundary in the Luleå area, northern Sweden: field and isotope geochemical evidence for a sharp terrane boundary. Precambrian Research, 96, 225–243. [https://doi.org/10.1016/S0301-9268\(99\)00011-X](https://doi.org/10.1016/S0301-9268(99)00011-X), 1999.
- 820 Naslund, H. R., Henríquez, F., Nyström, J. O., Vivallo, W., and Dobbs, F. M.: Magmatic iron ores and associated mineralisation: Examples from the Chilean High Andes and Coastal Cordillera, in: Hydrothermal Iron Oxide-Copper-Gold & Related Deposits: A Global Perspective, vol. 2, PCG Publishing, Adelaide, 207–226, 2002.
- Nyström, J. O. and Henríquez, F.: Magmatic features of iron ores of the Kiruna type in Chile and Sweden: ore textures and magnetite geochemistry, Economic Geology, 89, 820–839. <https://doi.org/10.2113/gsecongeo.89.4.820>, 1994.
- 825 Öhlander, B., Skiöld, T., Elming, S.-Å., Claesson, S., and Nisca, D. H.: Delineation and character of the Archaean–Proterozoic boundary in northern Sweden, Precambrian Res., 64, 67–84. [https://doi.org/10.1016/0301-9268\(93\)90069-E](https://doi.org/10.1016/0301-9268(93)90069-E), 1993.
- Parák, T.: The origin of the Kiruna iron ores. C. Davidsons Boktryckeri AB, Stockholm, 209 pp., 1975.
- Perdahl, J.-A. and Frietsch, R.: Petrochemical and petrological characteristics of 1.9 Ga old volcanics in northern Sweden, Precambrian Res., 64, 239–252. [https://doi.org/10.1016/0301-9268\(93\)90079-H](https://doi.org/10.1016/0301-9268(93)90079-H), 1993.
- 830 Pharaoh, T. C. and Pearce, J. A.: Geochemical evidence for the geotectonic setting of early Proterozoic metavolcanic sequences in Lapland, Precambrian Res., 25, 283–308. [https://doi.org/10.1016/0301-9268\(84\)90037-8](https://doi.org/10.1016/0301-9268(84)90037-8), 1984.
- del Real, I., Reich, M., Simon, A. C., Deditius, A., Barra, F., Rodríguez-Mustafa, M. A., Thompson, J. F. H., and Roberts, M. P.: Formation of giant iron oxide-copper-gold deposits by superimposed, episodic hydrothermal pulses, Commun Earth Environ, 2, 192. <https://doi.org/10.1038/s43247-021-00265-w>, 2021.
- 835 Reich, M., Simon, A. C., Deditius, A., Barra, F., Chryssoulis, S., Lagas, G., Tardani, D., Knipping, J., Bilenker, L., Sanchez-Alfaro, P., Roberts, M. P., and Munizaga, R.: Trace element signature of pyrite from the Los Colorados iron oxide-apatite (IOA) deposit, Chile: a missing link between Andean IOA and iron oxide copper-gold systems?. Economic Geology and the Bulletin of the Society of Economic Geologists, 111, 743–761. <https://doi.org/10.2113/econgeo.111.3.743>, 2016.
- Reich, M., Simon, A. C., Barra, F., Palma, G., Hou, T., and Bilenker, L. D.: Formation of iron oxide-apatite deposits, Nat Rev Earth Environ, 3, 758–775. <https://doi.org/10.1038/s43017-022-00335-3>, 2022.
- 840 Romer, R. L.: U-Pb systematics of stilbite-bearing low-temperature mineral assemblages from the Malmberget iron ore, northern Sweden. Geochemica et Cosmochimica Acta, 60, 1951–1961, 1996.
- Romer, R. L., Martinsson, O., and Perdahl, J. A.: Geochronology of the Kiruna iron ores and hydrothermal alterations, Economic Geology, 89, 1249–1261. <https://doi.org/10.2113/gsecongeo.89.6.1249>, 1994.
- 845 Sarlus, Z., Andersson, U. B., Bauer, T. E., Wanhainen, C., Martinsson, O., Nordin, R., and Andersson, J. B. H.: Timing of plutonism in the Gällivare area: implications for Proterozoic crustal development in the northern Norrbotten ore district, Sweden, Geol. Mag., 155, 1351–1376. <https://doi.org/10.1017/S0016756817000280>, 2018.

Sarlus, Z., Andersson, U. B., Martinsson, O., Bauer, T. E., Wanhainen, C., Andersson, J. B. H., and Whitehouse, M. J.: Timing and origin of the host rocks to the MalMBERGET iron oxide-apatite deposit, Sweden, *Precambrian Res.*, 342, 105652, <https://doi.org/10.1016/j.precamres.2020.105652>, 2020.

850 Sillitoe, R. H.: Iron oxide-copper-gold deposits: an Andean view, *Mineralium Deposita*, 38, 787–812, <https://doi.org/10.1007/s00126-003-0379-7>, 2003.

855 Simon, A. C., Knipping, J., Reich, M., Barra, F., Deditius, A. P., Bilinker, L., and Childress, T.: Kiruna-Type Iron Oxide-Apatite (IOA) and Iron Oxide Copper-Gold (IOCG) Deposits Form by a Combination of Igneous and Magmatic-Hydrothermal Processes: Evidence from the Chilean Iron Belt, in: *Metals, Minerals, and Society*, Society of Economic Geologists (SEG), <https://doi.org/10.5382/SP.21.06>, 2018.

Skelton, A., Mansfeld, J., Ahlin, S., Lundqvist, T., Linde, J., and Nilsson, J.: A compilation of metamorphic pressure-temperature estimates from the Svecofennian province of eastern and central Sweden. *GFF*, 140, 1–10, <https://doi.org/10.1080/11035897.2017.1414074>, 2018.

860 Skiöld, T.: Implications of new U-Pb zircon chronology to early Proterozoic crustal accretion in northern Sweden, *Precambrian Res.*, 38, 147–164, [https://doi.org/10.1016/0301-9268\(88\)90089-7](https://doi.org/10.1016/0301-9268(88)90089-7), 1988.

Skirrow, R. G.: Iron oxide copper-gold (IOCG) deposits – a review (part 1): settings, mineralogy, ore geochemistry, and classification, *Ore Geol. Rev.*, 104569, <https://doi.org/10.1016/j.oregeorev.2021.104569>, 2021.

865 Skyttä, P., Bauer, T. E., Tavakoli, S., Hermansson, T., Andersson, J., and Weihed, P.: Pre-1.87Ga development of crustal domains overprinted by 1.87Ga transpression in the Palaeoproterozoic Skellefte district, Sweden, *Precambrian Res.*, 206–207, 109–136, <https://doi.org/10.1016/j.precamres.2012.02.022>, 2012.

Skyttä, P., Määttä, M., Palsatech Oy, Piippo, S., Kara, J., Käpyaho, A., Heilimo, E., and O'Brien, H.: Constraints over the age of magmatism and subsequent deformation for the Neoproterozoic Kukkola Gneiss Complex, northern Fennoscandia, *Bull Geol Soc Finland*, 92, 19–38, <https://doi.org/10.17741/bgsf/92.1.002>, 2020.

870 Skyttä, P., Piippo, S., Kloppenburg, A., and Corti, G.: 2.45 Ga break-up of the Archaean continent in Northern Fennoscandia: Rifting dynamics and the role of inherited structures within the Archaean basement, *Precambrian Research*, 324, 303–323, <https://doi.org/10.1016/j.precamres.2019.02.004>, 2019.

Smith, M., Coppard, J., Herrington, R., and Stein, H.: The Geology of the Rakkurijärvi Cu-(Au) Prospect, Norrbotten: A New Iron Oxide-Copper-Gold Deposit in Northern Sweden, *Economic Geology*, 102, 393–414, <https://doi.org/10.2113/gsecongeo.102.3.393>, 2007.

875 Smith, M., Coppard, J., and Herrington, R.: The geology of the Rakkurijärvi copper-prospect, Norrbotten county, Sweden, in: *Hydrothermal Iron Oxide Copper-Gold and Related Deposits: A Global Perspective*, vol. v.4-Advances in the Understanding of IOCG Deposits, edited by: Porter, T. M., PGC Publishing, Adelaide, 427–440, 2010.

880 Smith, M. P., Storey, C. D., Jeffries, T. E., and Ryan, C.: In situ U-Pb and Trace Element Analysis of Accessory Minerals in the Kiruna District, Norrbotten, Sweden: New Constraints on the Timing and Origin of Mineralization, *Journal of Petrology*, 50, 2063–2094, <https://doi.org/10.1093/petrology/egp069>, 2009.

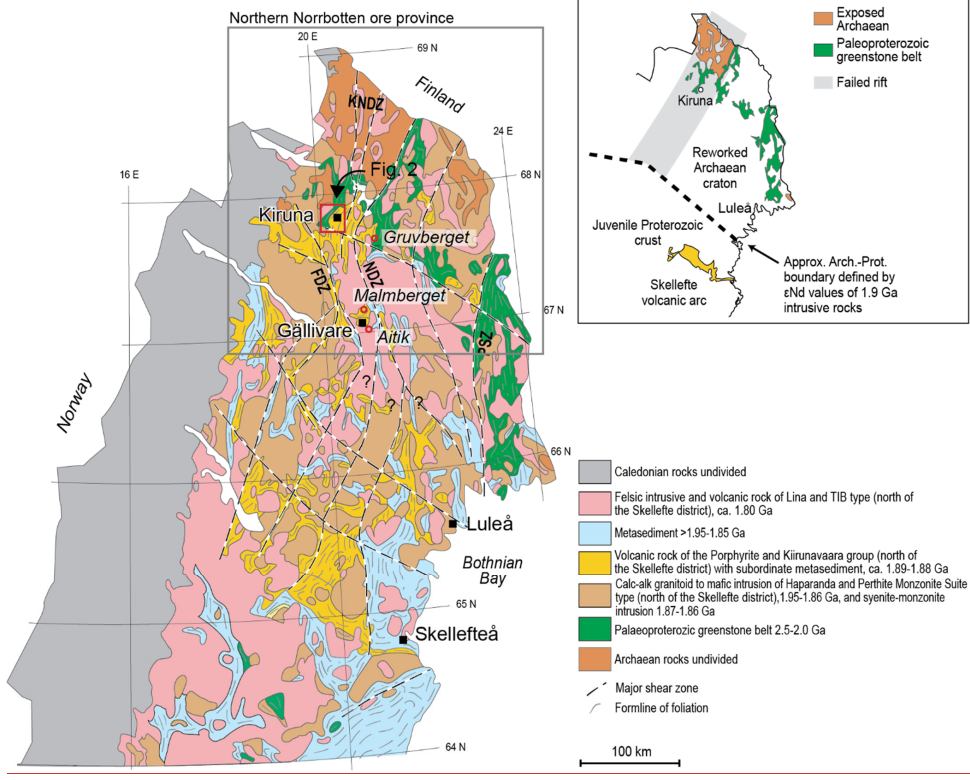
Storey, C. D., Smith, M. P., and Jeffries, T. E.: In situ LA-ICP-MS U-Pb dating of metavolcanics of Norrbotten, Sweden: Records of extended geological histories in complex titanite grains, *Chemical Geology*, 240, 163–181, <https://doi.org/10.1016/j.chemgeo.2007.02.004>, 2007.

Formatted: English (United Kingdom)

- 885 Tornos, F.: Magnetite-Apatite and IOCG deposits formed by magmatic-hydrothermal evolution of complex calc-alkaline melts, in: Eleventh Biennial SGA Meeting, Let's talk ore deposits, Antofagasta, Chile, 26–28, 2011.
- Tornos, F., Velasco, F., and Hanchar, J. M.: The Magmatic to Magmatic-Hydrothermal Evolution of the El Laco Deposit (Chile) and Its Implications for the Genesis of Magnetite-Apatite Deposits, *Economic Geology*, 112, 1595–1628, <https://doi.org/10.5382/econgeo.2017.4523>, 2017.
- 890 Troll, V. R., Weis, F. A., Jonsson, E., Andersson, U. B., Majidi, S. A., Högdahl, K., Harris, C., Millet, M.-A., Chinnasamy, S. S., Kooijman, E., and Nilsson, K. P.: Global Fe–O isotope correlation reveals magmatic origin of Kiruna-type apatite-iron-oxide ores, *Nat Commun*, 10, 1712, <https://doi.org/10.1038/s41467-019-09244-4>, 2019.
- Velasco, F., Tornos, F., and Hanchar, J. M.: Immiscible iron- and silica-rich melts and magnetite geochemistry at the El Laco volcano (northern Chile): Evidence for a magmatic origin for the magnetite deposits, *Ore Geol. Rev.*, 79, 346–366, <https://doi.org/10.1016/j.oregeorev.2016.06.007>, 2016.
- 895 Vollmer, F. W., Wright, S. F., and Hudleston, P. J.: Early deformation in the Svecokarelian greenstone belt of the Kiruna iron district, northern Sweden, *Geologiska Föreningen i Stockholm Förhandlingar*, 106, 109–118, <https://doi.org/10.1080/11035898409454620>, 1984.
- 900 Wanhainen, C., Billström, K., Martinsson, O., Stein, H., and Nordin, R.: 160 Ma of magmatic/hydrothermal and metamorphic activity in the Gällivare area: Re–Os dating of molybdenite and U–Pb dating of titanite from the Aitik Cu–Au–Ag deposit, northern Sweden, *Miner Deposita*, 40, 435–447, <https://doi.org/10.1007/s00126-005-0006-x>, 2005.
- Wanhainen, C., Broman, C., Martinsson, O., and Magnor, B.: Modification of a Palaeoproterozoic porphyry-like system: Integration of structural, geochemical, petrographic, and fluid inclusion data from the Aitik Cu–Au–Ag deposit, northern Sweden, *Ore Geol. Rev.*, 48, 306–331, <https://doi.org/10.1016/j.oregeorev.2012.05.002>, 2012.
- 905 Weihed, P. and Williams, P. J.: Metallogeny of the northern Fennoscandian Shield: a set of papers on Cu–Au and VMS deposits of northern Sweden, *Miner Deposita*, 40, 347–350, <https://doi.org/10.1007/s00126-005-0022-x>, 2005.
- Weihed, P., Billström, K., Persson, P.-O., and Weihed, J. B.: Relationship between 1.90–1.85 Ga accretionary processes and 1.82–1.80 Ga oblique subduction at the Karelian craton margin, Fennoscandian Shield, *GFF*, 124, 163–180, <https://doi.org/10.1080/11035890201243163>, 2002.
- 910 Welin, E.: The depositional evolution of the Svecofennian supracrustal sequence in Finland and Sweden, *Precambrian Res.*, 35, 95–113, [https://doi.org/10.1016/0301-9268\(87\)90047-7](https://doi.org/10.1016/0301-9268(87)90047-7), 1987.
- Westhues, A., Hanchar, J. M., Whitehouse, M. J., and Martinsson, O.: New Constraints on the Timing of Host-Rock Emplacement, Hydrothermal Alteration, and Iron Oxide-Apatite Mineralization in the Kiruna District, Norrbotten, Sweden, *Economic Geology*, 111, 1595–1618, <https://doi.org/10.2113/econgeo.111.7.1595>, 2016.
- 915 Westhues, A., Hanchar, J. M., Voisey, C. R., Whitehouse, M. J., Rossman, G. R., and Wirth, R.: Tracing the fluid evolution of the Kiruna iron oxide apatite deposits using zircon, monazite, and whole rock trace elements and isotopic studies, *Chemical Geology*, 466, 303–322, <https://doi.org/10.1016/j.chemgeo.2017.06.020>, 2017.
- Williams, P. J., Barton, M. D., Johnson, D. A., Fontboté, L., Haller, A. de, Mark, G., Oliver, N. H. S., and Marschik, R.: Iron Oxide Copper-Gold Deposits - Geology, Space-Time Distribution, and Possible Modes of Origin, in: *One Hundredth Anniversary Volume, Society of Economic Geologists*, Littleton, USA, 371–405, <https://doi.org/10.5382/AV100.13>, 2005.

- 920 Witschard, F.: The geological and tectonic evolution of the Precambrian of northern Sweden - A case for basement reactivation?, *Precambrian Res.*, 23, 273–315, [https://doi.org/10.1016/0301-9268\(84\)90047-0](https://doi.org/10.1016/0301-9268(84)90047-0), 1984.
- Wright, S.: Early Proterozoic Deformational History of the Kiruna District, Northern Sweden, Doctoral Thesis, University of Minnesota, 170 pp., 1988.
- 925 Wyborn, L. A. I., Heinrich, C. A., and Jaques, A. L.: Australian Proterozoic Mineral Systems: Essential Ingredients and Mappable Criteria, in: Australasian Institute of Mining and Metallurgy Publication Series, the AusIMM Annual Conference, Darwin, Australia, 109–115, 1994.
- Bauer, T. E. and Andersson, J. B. H.: Structural controls on Cu-Au mineralization in the Svappavaara area, northern Sweden: The northern continuation of the Nautanen IOCG system (paper II), in: Paleoproterozoic deformation in the Kiruna-Gällivare area in northern Norrbotten, Sweden: Setting, character, age, and control of iron-oxide-apatite deposits (PhD Thesis), edited by: Andersson, J. B. H., Luleå University of Technology, Luleå, Sweden, 1–15, 2021.
- 930 Bauer, T. E., Andersson, J. B. H., Sarlus, Z., Lund, C., and Kearney, T.: Structural Controls on the Setting, Shape, and Hydrothermal Alteration of the Malmberget Iron-Oxide-Apatite Deposit, Northern Sweden, *Econ Geol.*, 113, 377–395, <https://doi.org/10.5382/econgeo.2018.4554>, 2018.
- Bergman, S., Kübler, L., and Martinsson, O.: Description of regional geological and geophysical maps of northern Norrbotten County (east of the Caledonian orogen), *Sveriges geologiska undersökning*, Uppsala, 110 pp., 2001.
- 935 Martinsson, O., Perdahl, J. A., and Bergman, J.: Greenstone and porphyry-hosted ore deposits in northern Norrbotten, *Nutek*, 1993.
- Skelton, A., Mansfeld, J., Ahlin, S., Lundqvist, T., Linde, J., and Nilsson, J.: A compilation of metamorphic pressure-temperature estimates from the Svecofennian province of eastern and central Sweden, *GFF*, 140, 1–10, <https://doi.org/10.1080/11035897.2017.1414074>, 2018.
- 940 Skyttä, P., Piippo, S., Kloppenburg, A., and Corti, G.: 2.45 Ga break-up of the Archaean continent in Northern Fennoscandia: Rifting dynamics and the role of inherited structures within the Archaean basement, *Precambrian Research*, 324, 303–323, <https://doi.org/10.1016/j.precamres.2019.02.004>, 2019.
- Weihed, P. and Williams, P. J.: Metallogeny of the northern Fennoscandian Shield: a set of papers on Cu-Au and VMS deposits of northern Sweden, *Miner Deposita*, 40, 347–350, <https://doi.org/10.1007/s00126-005-0022-x>, 2005.
- 945 Wyborn, L. A. I., Heinrich, C. A., and Jaques, A. L.: Australian Proterozoic Mineral Systems: Essential Ingredients and Mappable Criteria, in: Australasian Institute of Mining and Metallurgy Publication Series, the AusIMM Annual Conference, Darwin, Australia, 109–115, 1994.

950



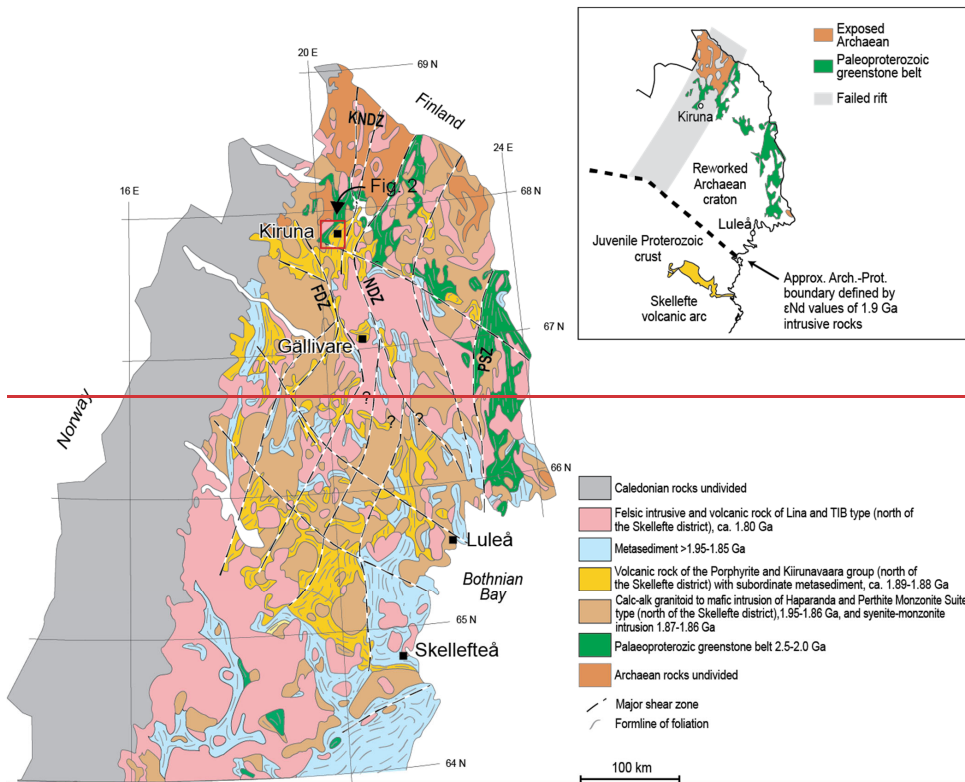
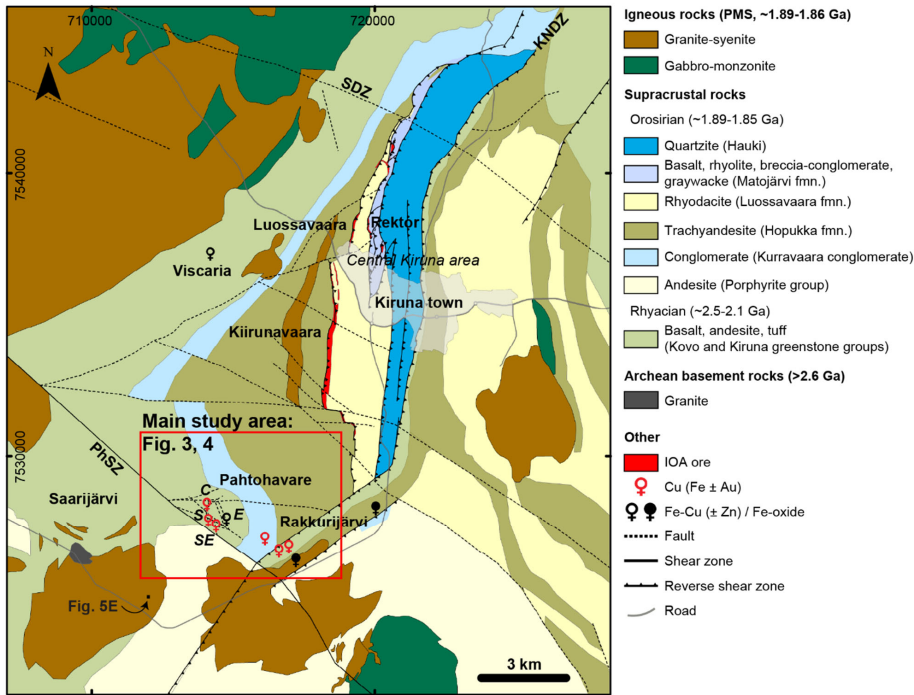
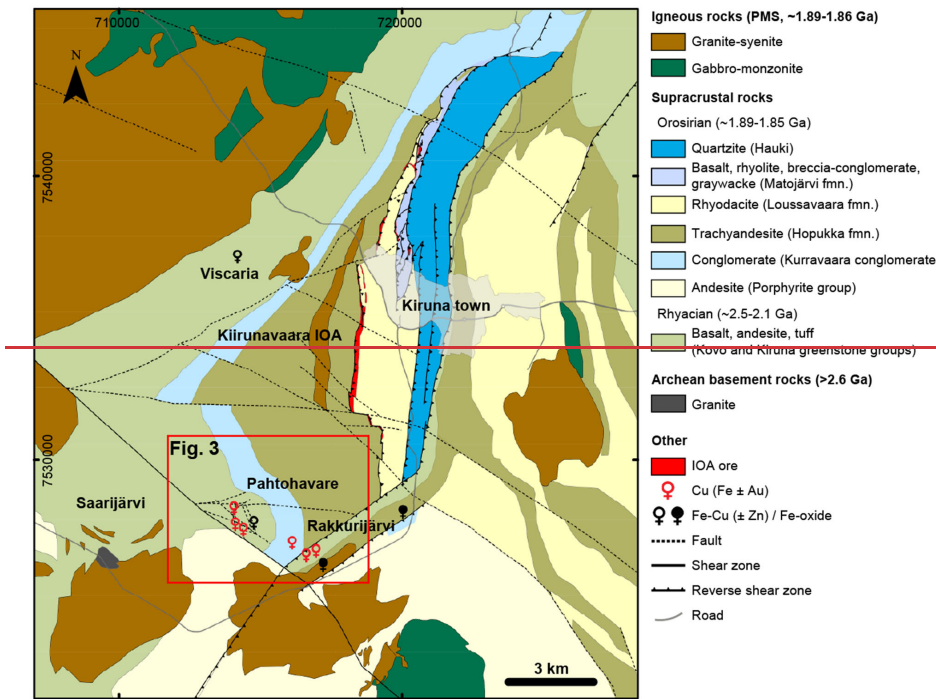


Figure 1: Geologic map of northern Sweden with both the Skellefte district and the northern Norrbotten ore province included. Inset shows approximate paleoboundary of the Archean craton defined by ϵNd values (Öhlander et al., 1993). FDZ = Fjällåsen deformation zone, KNDZ = Kiruna-Naimakka deformation zone, NDZ = Nautanen deformation zone, PSZ = Pajala shear zone. Modified after Bauer et al. (2022), Weihed and Williams (2005), and Bauer and Andersson (2021).

955





960 Figure 2: Geologic map of the Kiruna mining district showing stratigraphy, structures, and igneous intrusions. Kiruna town is marked in transparent gray. Cu (Fe ± Au), Fe-Cu (± Zn), and Fe-oxide occurrences are shown as well as local area names. Pahtohavare deposits: C = Central, E = Eastern, S = Southern, SE = Southeastern, KNDZ = Kiruna-Naimakka deformation zone, PhSZ = Pahtohavare shear zone, SDZ = Svappavaara deformation zone. Modified after Martinsson et al. (1993) and Andersson et al. (2021). Coordinate system in SWEREF99.

965

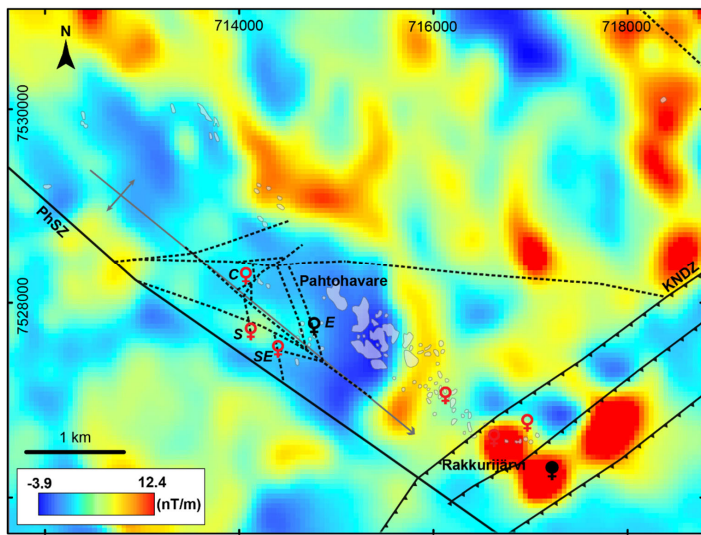
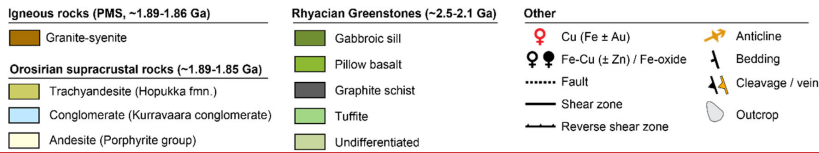
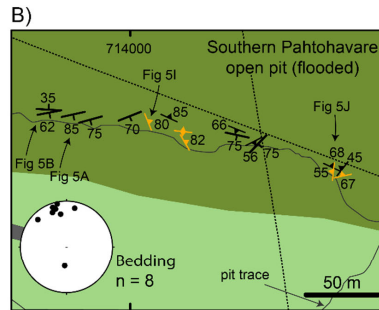
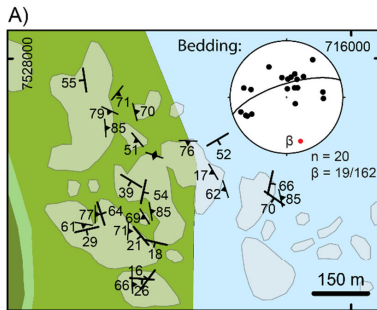
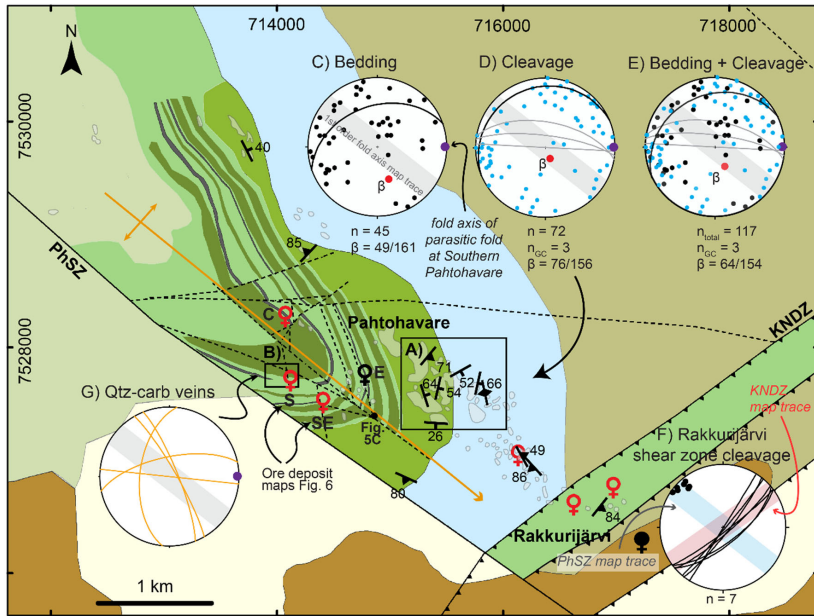


Figure 3: Aeromagnetic anomaly map showing the vertical gradient of the total magnetic intensity anomaly upward continued to 150 m. Symbology as in Fig. 4. Data source: Geological Survey of Sweden. Data processing by T. Rasmussen.

Formatted: Caption



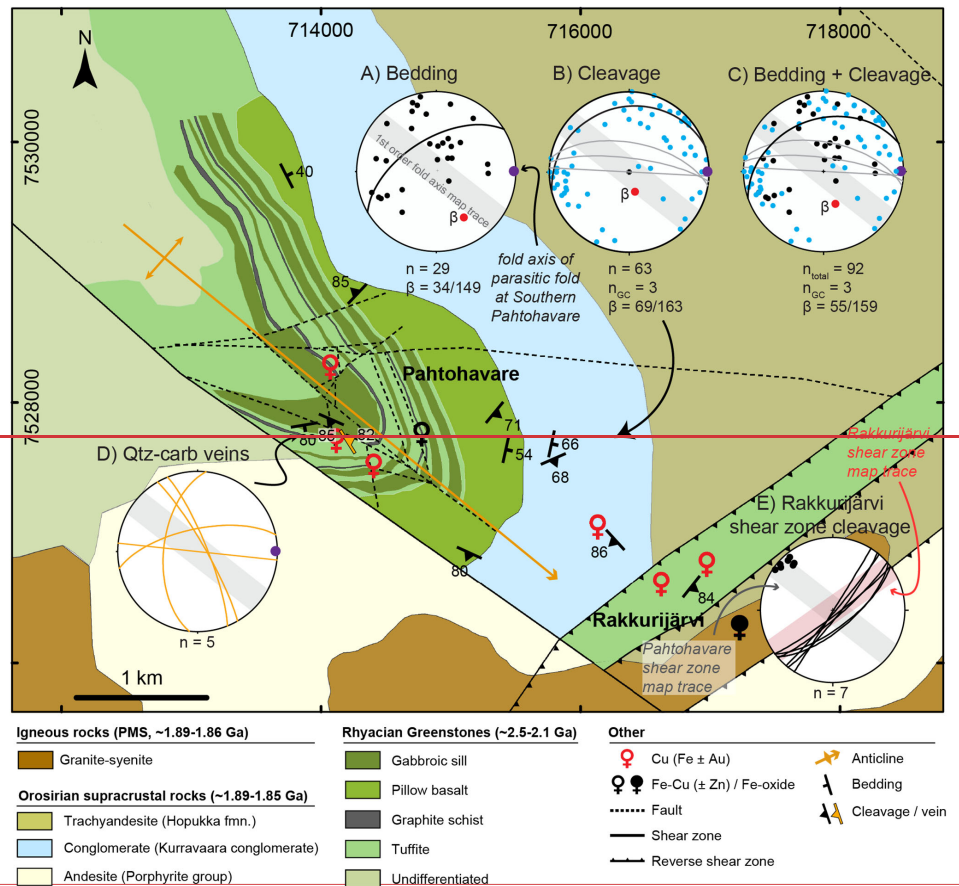
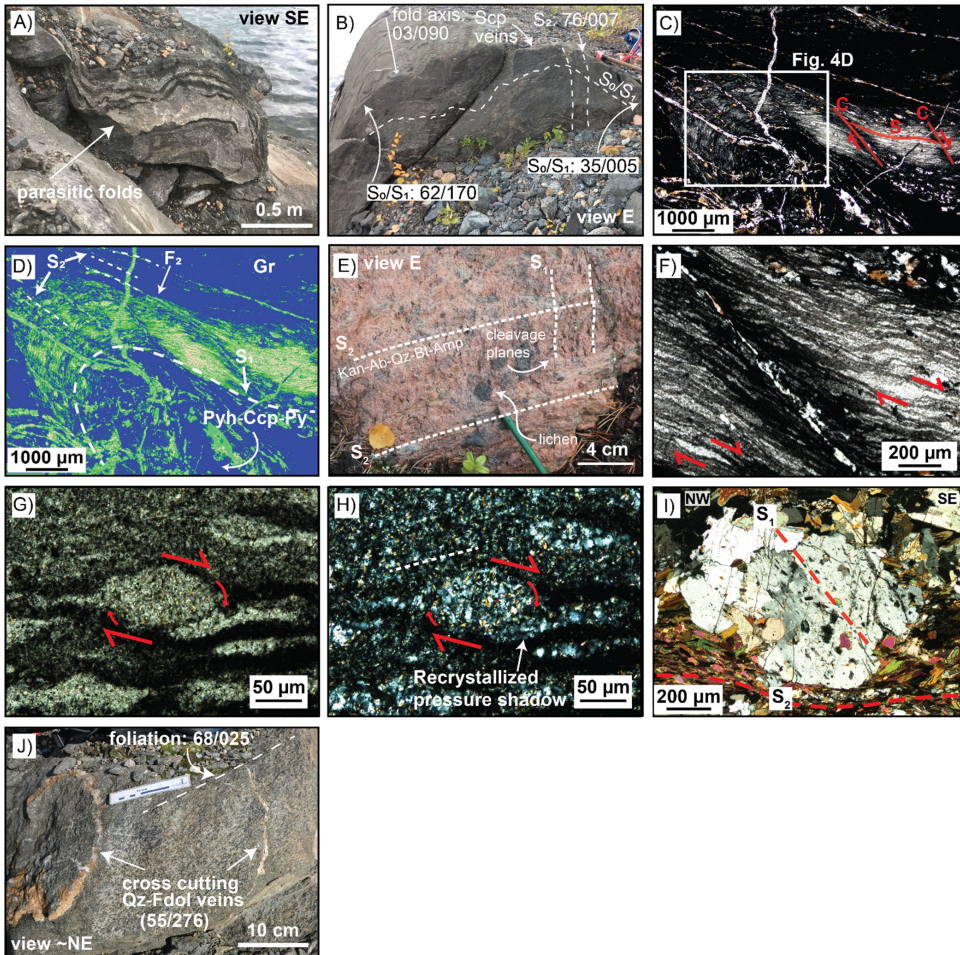


Figure 34: Geologic map of the Pahtohavare and Rakkurijärvi areas with structural results. **A) Structural measurements from a densely outcropping area in the northern limb of the anticline. Where multiple measurements existed at the same locality, the visualization was simplified to show the main orientations. A lower hemisphere, equal area stereographic projection of bedding planes is shown for this area, B) Structural measurements from the Southern Pahtohavare deposit open pit with a stereographic projection of bedding planes, C-E) Lower hemisphere, equal area stereographic projections of all of the structures in the Pahtohavare and Rakkurijärvi area showing A) bedding (C), B) cleavage (D), C) and combined bedding and cleavage, respectively (E), D-E) Cleavage measurements near the Rakkurijärvi shear zone quartz-carbonate vein orientations at Southern Pahtohavare open pit, E-G) Quartz-carbonate vein orientations at Southern Pahtohavare open pit cleavage measurements near the Rakkurijärvi shear zone. Gray band shows the apparent fold axis map trace. Gray great circles (GC) indicate axial subparallel veins to the parasitic fold (fold axis = purple dot) at Pahtohavare southern open pit. PhSZ = Pahtohavare shear zone, KNDZ = Kiruna-Naimakka**

deformation zone, S = Southern, SE = Southeastern, C = Central, E = Eastern Pahtohavare deposits. Modified after Martinsson et al. (1993) and Martinsson (1997). Coordinate system in SWEREF99.



985

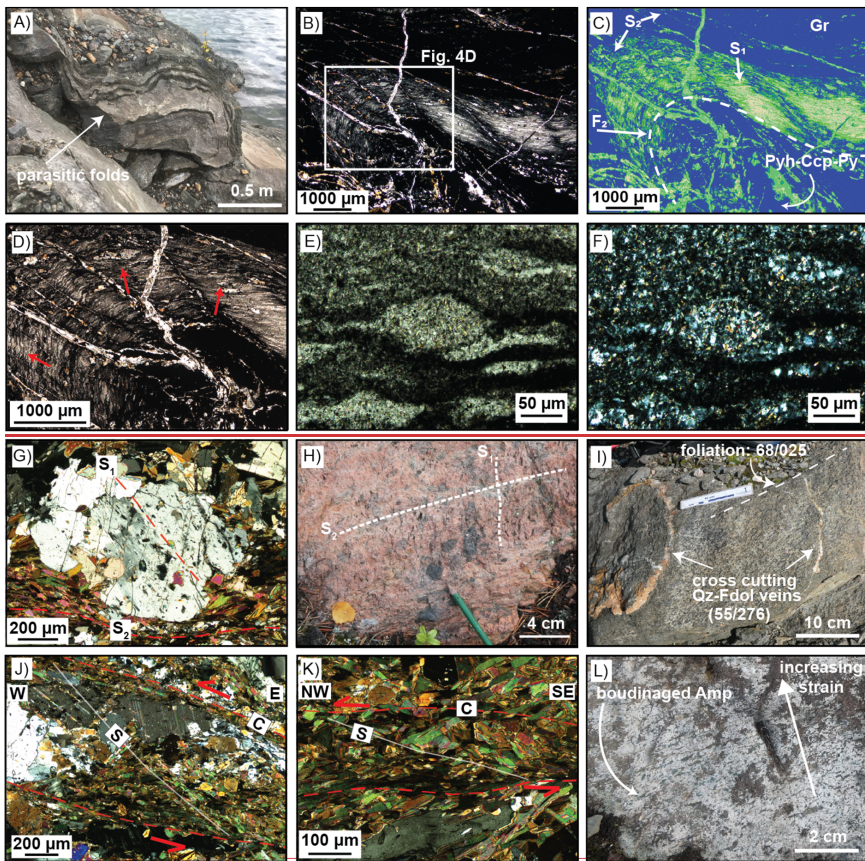


Figure 54: Photographs of structural features in the Pahtohavare-Rakkurijärvi areas. A-B) Parasitic folds in tuffitic layers as a part of a bigger fold system. Photos taken at Pahtohavare Southern open pit. View southeast. BC) Micrograph of a micro-scale fold in graphitic schist from drill core near the Eastern Pahtohavare deposit showing pseudo-mylonitic S-C fabric. Photo in plane polarized light. Full thin section micrographs in plane polarized and reflected light can be found in S2 and S3. CD) False color image of graphitic schist in 4B-5C highlighting showing S₁, F₂, S₂, and F₂, and remobilized chalcopyrite, pyrite, and pyrrhotite occur in the fold hinge and in the spaced axial planar cleavage. E) Granitic intrusion 2.5 km SW of Pahtohavare showing two directions of tectonic cleavage. DE) Plane polarized light image of the hinge zone of the graphite schist in 5C, showing asymmetric sigmoidal clasts with dextral sense of shear. EG) Plane polarized light of an asymmetric sigmoidal clast from the graphite schist in 5C with recrystallized pressure shadows showing non-coaxial strain. FH) Cross polarized light (XPL) of the same clast. GI) Scapolite porphyroblast showing preserved foliation trails (S₁) and wrapped by a foliation defined by biotite (S₂). H) Granitic intrusion SW of Pahtohavare showing two directions of tectonic cleavage. IJ) Foliated mafic sill with Qtz-Fdol veins cross cutting at a high angle at Pahtohavare Southern open pit. View northeast. JK) S-C fabric in an oriented sample from a shear band in Pahtohavare Southern open pit showing a sinistral sense of shear. XPL. L) Strain partitioning of amphibole seen in outcrop scale in Rakkurijärvi.

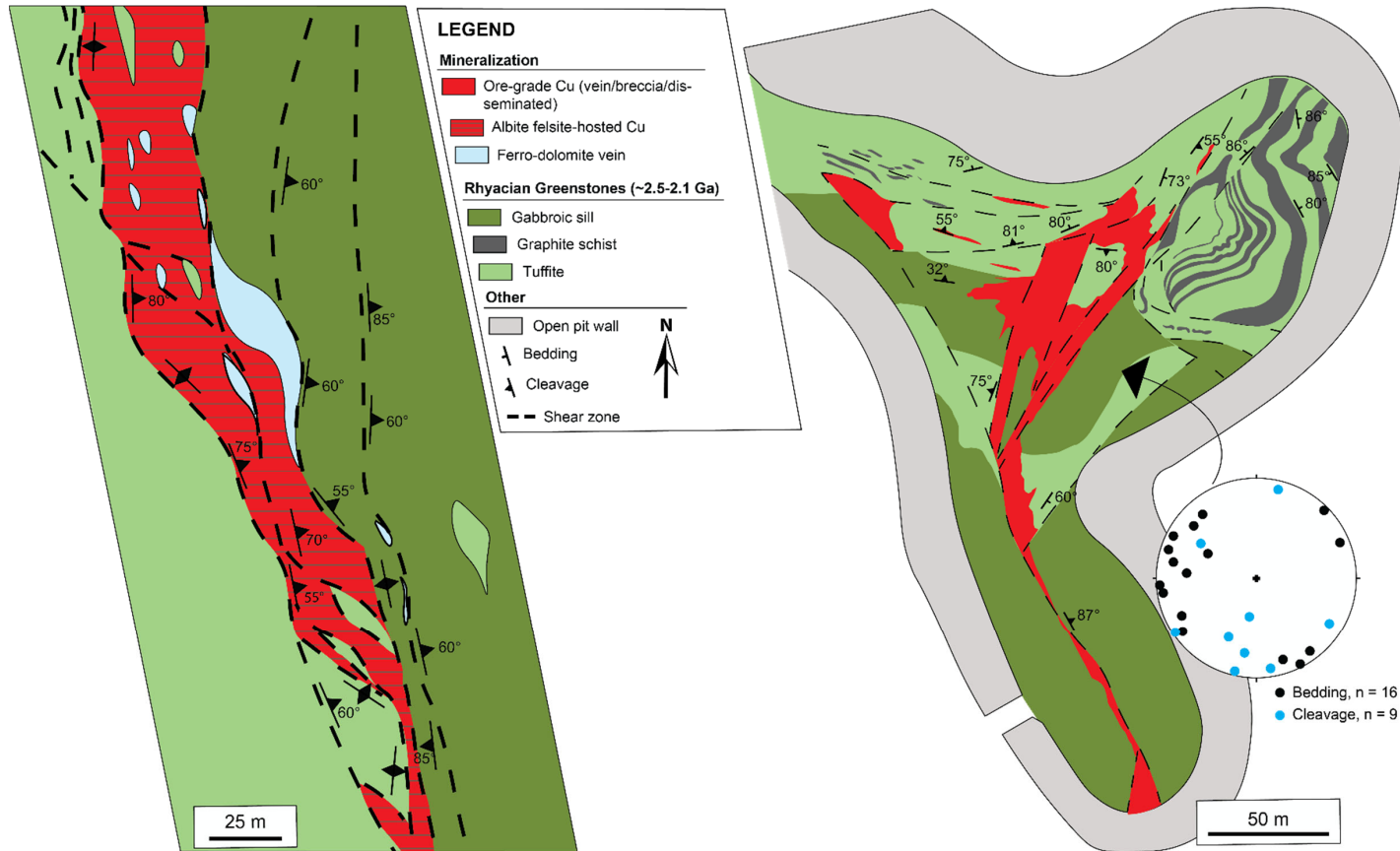
Formatted: Font color: Auto

Formatted: Subscript

000 ~~Weakly strained amphibole occurs at the bottom of the outcrop and boudinaged amphibole grains occur towards the top. View towards east. Structural measurements: dip/dip azimuth. Gr = graphite, Scp = scapolite, Pyh = pyrrhotite, Ccp = chalcopyrite, Py = pyrite, Kan = K-feldspar, Ab = albite, Qz = quartz, Bt = biotite, Amp = amphibole, Fdol = ferrodolomite, ~~Amp = amphibole~~.~~

A) Southern Pahtohavare, 300 m level

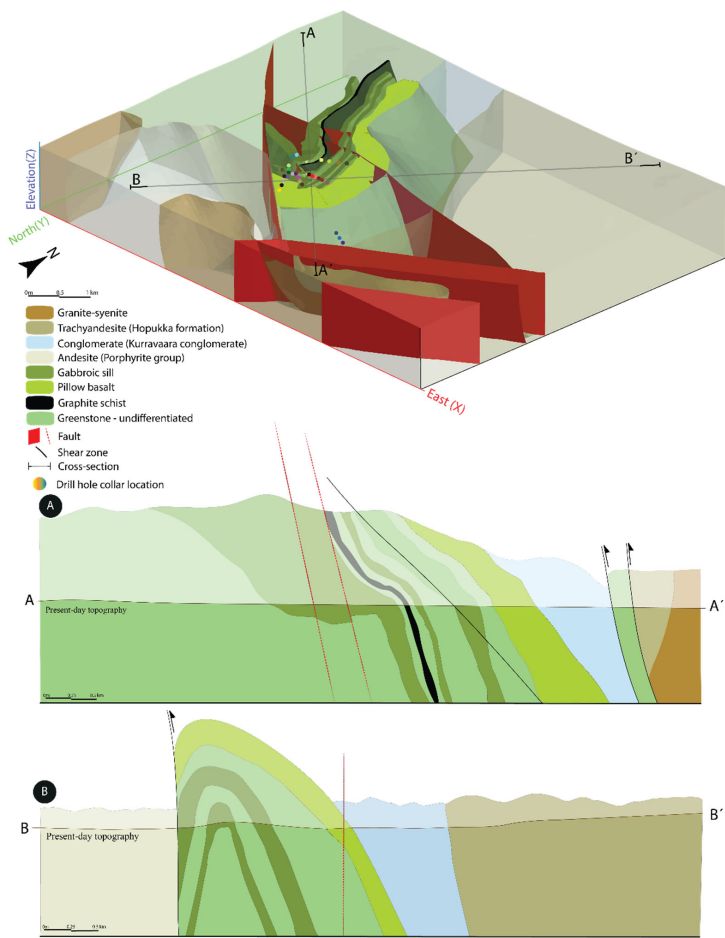
B) Southeastern Pahtohavare open pit



1005 **Figure 6: A) A mine level map at 300 m of the Southern Pahtohavare deposit showing albite felsite hosted Cu in a structurally-controlled position. The**
 1010 **construction of the mine level map was done for resource estimates during the 1990s by utilizing vertical cross sections from profiles every ten meters**
along the strike of the ore body with 3 to 5 inclined drillholes in each profile intersecting the ore body at various depths. Geological contacts and structures
have been interpolated from the vertical cross sections. Dipping of contacts and structures are estimated from the cross sections and are not based on
actual structural measurements. B) The Southeastern Pahtohavare open pit showing both the stratabound and discordant ore zones. Structural
measurements were acquired during mapping in the 1990s.

Formatted: Caption

Formatted: English (United Kingdom)



Formatted: Top: 0.39", Bottom: 0.93", Footer distance from edge: 0.51"

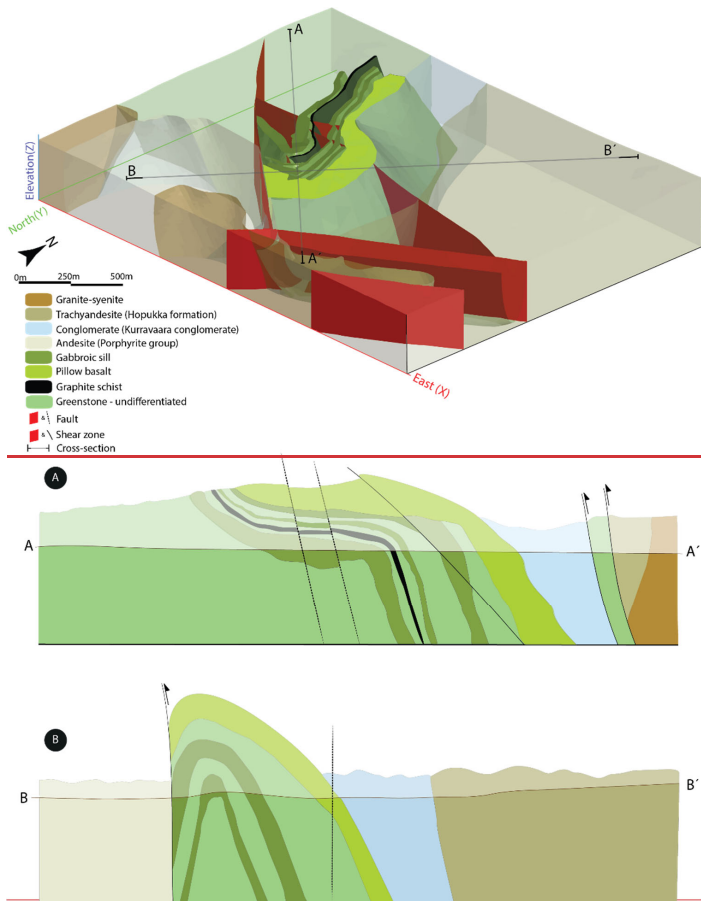
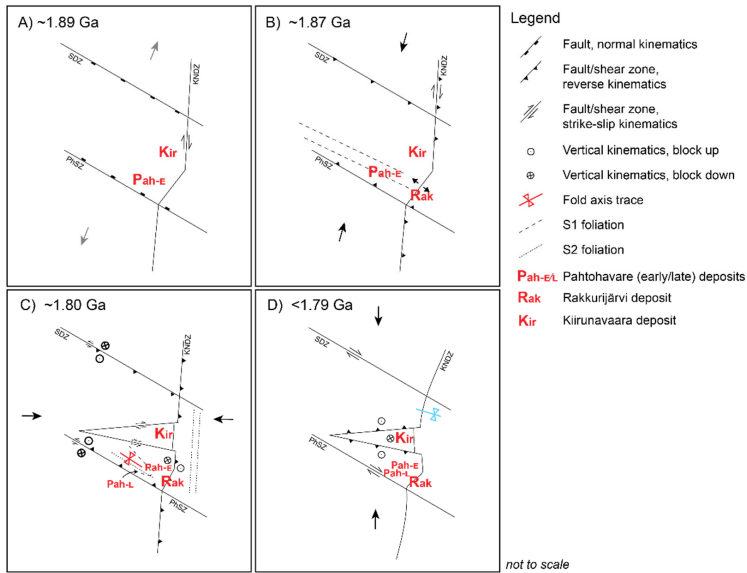


Figure 75: Local 3D model (viewed from above and SE towards the NW) and conceptual cross-sections of the southern Kiruna mining district, showing the major lithological boundaries, faults, and shear-zones. The geological 3D model is built based on the local geological map, structural measurements, and lithological drill hole logs (drill hole numbers and coordinates can be found in supplementary Table S1), and the 3D model highlights the Pahtohavare F₂ fold by utilizing different transparency levels of the adjacent lithological units. The conceptual cross-sections interpreted from the 3D model and structural data in this study highlight the geometry of the fold and the relationship between brittle-ductile structures and local lithostratigraphic units from, A) NW-SE orientation, and B) SW-NE orientation. An interactive 3D model is available in S4.

Formatted: Not Highlight



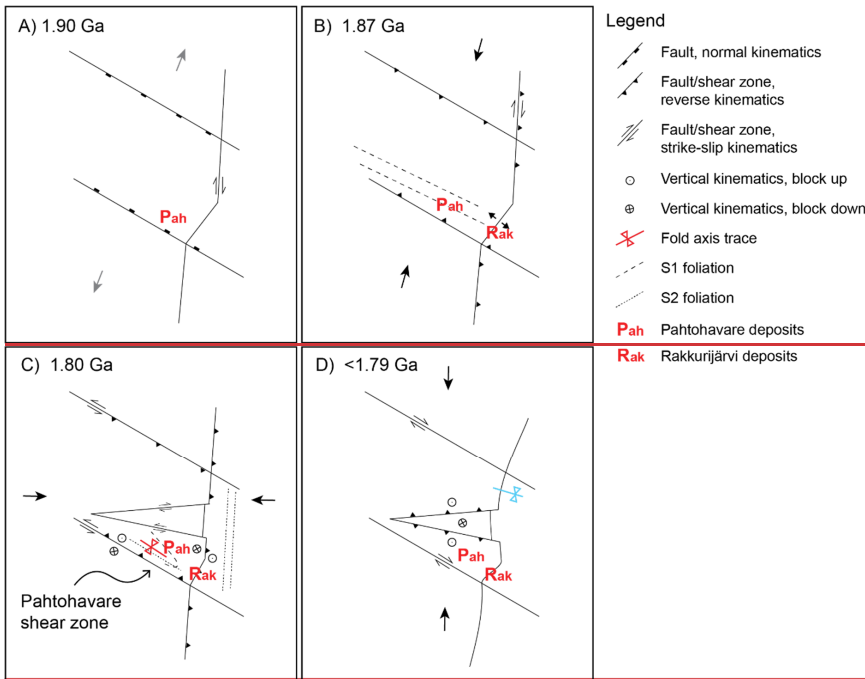
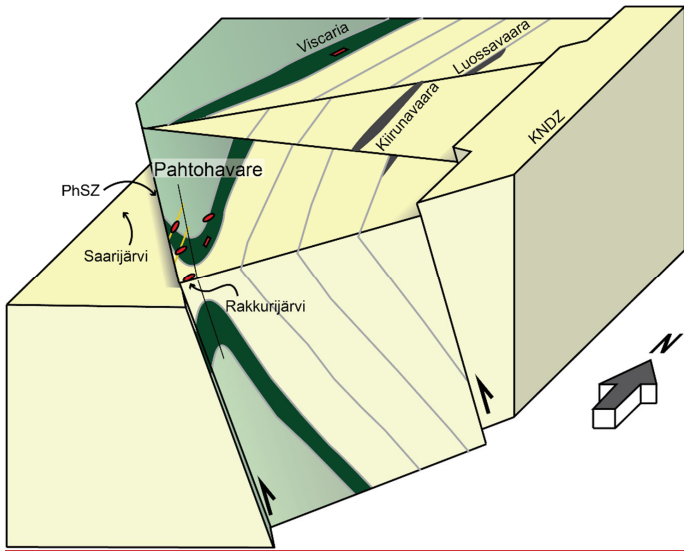


Figure 86: A proposal for the structural framework for the Kiruna mining district. A) The onset of the Svecofennian orogeny and back arc extension forms and/or reutilizes preexisting normal faults, additional transtensional faults form. The earliest ca. 2.1 Ga Pahtohavare syngenetic deposit (Eastern, $P_{ah,e}$) has already formed and the Kiirunavaara IOA deposit forms. B) NE-SW crustal shortening from the early Svecofennian orogeny reactivates preexisting faults structures, forming transpressional shear zones and dilatational jogs. The Rakkurijärvi IOCG forms (Rak). Early S_1 fabric develops in the southern Kiruna mining district, C) Late orogenic E-W crustal shortening and basin inversion occurs. Stratigraphy in the Pahtohavare-Rakkurijärvi area is folded and S_2 foliation develops. Strong strain partitioning occurs with S_2 fabric forming along shear zones in the central Kiruna area. Both brittle and ductile structures form. The late epigenetic Pahtohavare deposits form ($P_{ah,l}$). D) N-S crustal shortening causes gentle refolding in the district and minor reactivation of preexisting structures occurs. SDZ = Svappavaara deformation zone, KNDZ = Kiruna-Naimakka deformation zone, PhSZ = Pahtohavare shear zone.

Formatted: Subscript

Formatted: Subscript

Formatted: English (United States)



035

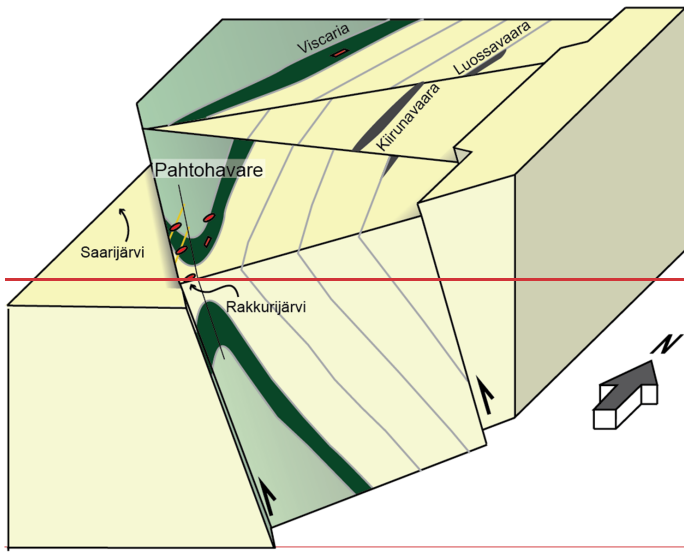


Figure 79: 3D conceptual model of the Pahtohavare area in the southern Kiruna mining district showing the oblique reverse NW-SE trending Pahtohavare shear zone and the resultant Pahtohavare F₂ fold. The axial surface is steeply dipping and the Pahtohavare epigenetic deposits are controlled by D₂ structures. Green colors denote older greenstone stratigraphy (ca. >2.1 Ga) and yellow colors denote ca. 1.92 Ga and younger stratigraphy. KNDZ = Kiruna-Naimakka deformation zone, PhSZ = Pahtohavare shear zone.

040

Supplementary material

S1. Geologic map showing all bedding and cleavage measurement localities, observation points, outcrop exposure, and collar locations of the drill holes used in the 3D model (Fig. 7) in the Pahtohavare-Rakkurijärvi area. Outcrop data from SGU.

045 S2. Plane polarized light gull thin section micrograph of a parasitic fold taken from drill core.

S3. Reflected light full thin section micrograph of a parasitic fold taken from drill core.

S4. Interactive 3D model of the southern Kiruna mining district (presented in Fig. 7), including faults, shear zones (partly covered by lithologies), and lithological boundaries (with 40% transparency).

Table S1. Legend for drill hole collar locations used in 3D model.

Formatted: Caption